

Changes in the frequency and intensity of extremes over Northeast Africa

Gebru Jember Endalew

De Bilt, 2007

PO Box 201
3730 AE De Bilt
Wilhelminalaan 10
De Bilt
The Netherlands
<http://www.knmi.nl>
Telephone +31(0)30-220 69 11
Telefax +31(0)30-221 04 07

Author: Gebru Jember Endalew



CHANGES IN THE FREQUENCY AND INTENSITY OF EXTREMES OVER NORTHEAST AFRICA

Gebru Jember Endalew ^{a,b,*}

Supervision: B. van den Hurk^c and G. J van Oldenborgh^c

^a National Meteorological Agency of Ethiopia, Addis Ababa, Ethiopia

^b Department of Meteorology, Wageningen University, Netherlands

^c Royal Netherlands Meteorological Institute, De Bilt, Netherlands

July 2007
KNMI

*Correspondence to: Gebru J. Endalew, National Meteorological Agency, P.O. Box 1090, Addis Ababa, Ethiopia; e-mail:gebru_j@yahoo.com

Table of contents:

| | |
|--|----|
| ABSTRACT | |
| 1. INTRODUCTION | 3 |
| 1.1 BACKGROUND | 3 |
| 1.2 RESEARCH QUESTION | 4 |
| 1.3 STRUCTURE OF THE REPORT | 4 |
| 2. SEASONS AND SEASONAL CLASSIFICATIONS | 5 |
| 2.1 WEATHER SYSTEMS AFFECTING ETHIOPIA | 6 |
| 2.2 ETHIOPIA RAINFALL AND GLOBAL TELECONNECTION FEATURES | 9 |
| 2.2.1 PACIFIC OCEAN | 9 |
| 2.2.2 ATLANTIC OCEAN | 11 |
| 2.2.3 INDIAN OCEAN | 11 |
| 3. DATA AND METHODOLOGY | 13 |
| 4. DATA ANALYSIS AND RESULTS | 14 |
| 4.1 JUNE TO SEPTEMBER | 14 |
| 4.1.1 TREND OF SYSTEMS THAT GOVERN THE RAINFALL ACTIVITY OVER THE REGION DURING THE EXTREME WET AND DRY DECADES | 17 |
| 4.2 MARCH TO MAY | 27 |
| 4.2.1 TREND OF SYSTEMS THAT GOVERN THE RAINFALL ACTIVITY OVER THE REGION DURING THE EXTREME WET AND DRY DECADES | 29 |
| 5. CLIMATE CHANGE | 32 |
| 6. DISCUSSION AND CONCLUSION | 35 |
| ACKNOWLEDGEMENT | 37 |
| REFERENCES | 38 |
| APPENDICES | 40 |

ABSTRACT

Climate of Northeastern Africa varies from humid to semi-arid with both abundant and scarce moisture. Hence, flooding and drought are frequent phenomena which have a direct impact on the agriculture, health, water and other socio-economic sectors of the region. Analysis for the expected changes in the frequency and intensity of extreme rainfall induced by climate change in Ethiopia is the aim of this study.

The Ethiopian area has been divided into three homogeneous rainfall regimes (Zone A-C). The seasonal classification of the region, especially over Ethiopia, is from February to May, June to September and October to January, called Belg, Kiremt and Bega, respectively. Here, more emphasis is given to the Kiremt and Belg seasons.

Anomalous wet and dry decades were identified using ERA-40 data. The condition of the main rain bearing systems during these decades has been assessed and from this result systems which favor more for the extremes have been detected. Among the systems that control the weather activity in the region are: Inter-tropical Convergence Zone (ITCZ), Tropical Easterly Jet (TEJ), East African Low Level Jet (EALLJ), El Niño-Southern Oscillation (ENSO) as well as Mascarena, St. Helena, Azores and Arabian High pressure systems. Then simulations from GFDL and CCCma were analyzed.

There is large decadal variability in the occurrence of extreme rainfall events. During the Kiremt season, 90-96% wet anomalies were mostly occurring in the 1958-1979 time range. The dry anomalous decades were mostly found in 1980-2001 for both zone-A and -B. During Belg, all the dry anomalies are in the third decade of March for zone-B. During April and May, most of the dry anomalies are in the first decade. For zone-C, most of the dry anomalies are in the third decade of March.

The sources of moisture, the means of transport and the dynamic conditions should be satisfied to have a wet anomaly. During the driest decades these conditions are not fulfilled. The future scenario runs from GFDL and CCCma indicate that both models have a consistent trend. However, as most models have limitations, even the seasonality is not well represented in both models.

Key words: Ethiopia, ERA-40, GFDL, CCCma, rainfall

1. INTRODUCTION

1.1 BACKGROUND

Northeastern Africa (with lat. 3° - 15° N and long. 33° - 48° E) climate varies from humid to semi-arid with abundant and scarce moisture. Hence, flooding and drought are nowadays most frequent phenomena which have a direct impact on the agriculture, health, water and other socio-economic sectors of the region. Looking for the expected climate change induced changes in the frequency and intensity of extreme rainfall will contribute in order to minimize the effects.

The seasonal classification of the region, especially over Ethiopia, is from February to May, June to September and October to January called Belg, Kiremt and Bega, respectively. Here, more emphasis is given to Belg (MAM) and Kiremt (JJAS) seasons and a detail on seasons is described in section 2 below.

Extremes were derived from gauge rainfall data (Korecha et al 2001). But the raingauge network is too sparse to produce reliable areal estimates. Using other sources like the Numerical Weather Prediction (NWP) model outputs overcome the drawback. These include the European Centre for Medium-Range Weather Forecast (ECMWF) data, which is now used in local operational application. For instance, it is used by the European Union Joint Research Council Monitoring of Agriculture with Remote Sensing (MARS) project at <http://agrifish.jrc.it/bulletins.htm> for bulletins related to famine early warning.

For this study, ECMWF 40 year re-analysis data (ERA-40) has been used. According to the evaluation of ERA-40 data by Tefera et al (2007), the spatial pattern of the JJAS rainfall climatology is captured well but exaggerates the peak in the northwestern and western Ethiopia. After assimilation of Satellite data from 1990's, this drawback has been reduced. Besides, the interannual variability is less well captured than the spatial and seasonal variability (Tefera et al, 2007). For the FMAM season, except in the extreme south of Ethiopia, inter-annual variability is shown better by ERA-40 (Tefera et al, 2007).

Identifying the anomalous wet and dry decades based on the ERA-40 data has been done. Then the condition of the main rain bearing systems during these decades has been integrated and from this result it has been detected which systems are related to the extremes. Then future scenario runs using the geophysical fluid dynamics laboratory (GFDL) and the Canadian Center for Climate modeling and analysis (CCCma) model have been analyzed.

1.2 RESEARCH QUESTION

Will climate change affect the intensity and frequency of extreme events in northeastern Africa?

- What large scale systems govern precipitation over NE Africa?
- Does precipitation change as expected?

1.3 STRUCTURE OF THE REPORT

After the introduction, Seasons and seasonal classifications are described in section 2. Data and methodology are presented in section 3; data analysis and results are in section 4. Climate change is in section 5 and Discussion and conclusions are given in section 6.

2. SEASONS AND SEASONAL CLASSIFICATIONS

In high and mid-latitudes, seasons are classified as winter, spring, summer and autumn, while in low latitudes they are categorized as wet and dry seasons. In the case of Ethiopia, the seasons are classified into three periods based on annual rainfall patterns. Hence, based on the mean annual and mean monthly rainfall distributions, the rainfall regimes are delineated and the types of seasons in Ethiopia are identified.

The central and most of the eastern half of the country (identified by letter A in Figure1) has two rainy periods and one dry period. The two rainy periods are locally known as Kiremt (June to September) and Belg (February to May), which are long and short rainy periods, respectively. The annual rainfall distribution over this region shows two peaks corresponding to the two rainy seasons, separated by a relatively short "dry" period. The dry period, which covers the rest of the year (i.e., October to January), is known as Bega.

The western part of Ethiopia, which is identified by the letter B in Figure1, has one rainfall peak during the year. As one goes toward the north within this region, the length of the rainy period (June to September) decreases due to the meridional migration of the ITCZ (Inter-Tropical Convergence Zone).

The southern and the southeastern parts of Ethiopia (the region identified by the letter C in (Figure 1) have two distinct dry periods (December to February and June to August). The temporal distribution of rainfall over these regions shows two distinct peaks separated by a well-marked dry period.

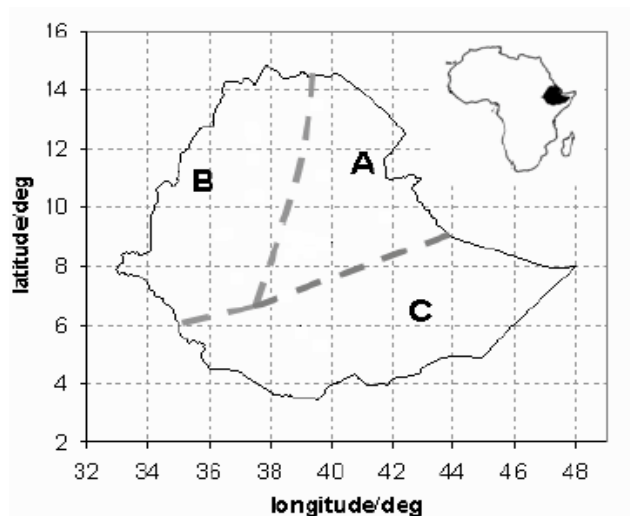


Figure 1: Map of study area. Dashed lines indicate regimes A, B and C. Inset shows location of Ethiopia with in Africa (Source: Bekele F. 1993)

Combining these regimes the year can be classified into four distinct seasons (Table 1). This is evidently true particularly for southern and southeastern portions (region C). However, for southwestern, western, central and northwestern Ethiopia (region A&B) only one dry and one long rainy season can be identified. Thus, the presence of four seasons, notably, winter (December-February), spring (march-May), summer (June-August) and autumn (September) are evident.

Table 1: Seasons and weather condition over the three regimes of Ethiopia

| | FEB | MAR | APR | MAY | JUN | JUL | AUG | SEP | OCT | NOV | DEC | JA |
|-------------|------|-----|-----|--------|-----|-----|-----|------|-----|-----|-----|----|
| Trad. Seas. | BELG | | | KIREMT | | | | BEGA | | | | |
| Regime A | Wet | | | | | Wet | | | Dry | | | |
| Regime B | Dry | | | | | Wet | | | Dry | | | |
| Regime C | Dry | Wet | | | Dry | | | Wet | | | Dry | |

In this study we give more emphasis for the extremes during JJAS for Zone-A and Zone-B then during MAM for Zone-B and Zone-C.

2.1 WEATHER SYSTEMS AFFECTING ETHIOPIA

Seasonal and annual rainfall variations in Ethiopia as well as the neighboring areas of the region are associated with the macro-scale pressure systems and monsoon flows (Tesfaye 1986, 1987; Hastenrath, 1991). Bekuretsion(1987) has indicated that the weather and climate of Ethiopia arises from the influence of tropical weather systems, like the Intertropical Convergence Zone (ITCZ), the

monsoon, easterly waves, etc., and quasi-stationary subtropical anticyclones of both northern and southern hemisphere. The interactions between the tropical and extratropical weather systems produce major active weather over the country, especially during the months of February to May (Northern Hemisphere Spring). The main weather bearing systems for the Bega, Belg and Kiremt seasons, respectively are discussed below.

1. During Bega (the dry season) the country predominantly falls under the influence of warm and cool northeasterly winds. These dry air masses originate either from the Saharan anticyclone or from the ridge of high pressure extending into Arabia from the large high over central Asia (Siberia). However, occasionally the northeasterly winds are interrupted when migrating low pressure systems originating in the Mediterranean area move southwards and interact with the tropical systems resulting into unseasonal rains over central and northern Ethiopia. Occasionally the development of the red Sea Convergence Zone (RSCZ) also produces rains over northeastern Ethiopia (Pedgley, 1966).

2. During Belg (the small rainy season) which is from March to May, the Arabian high moves towards the northern Arabian Sea. When it is pushed over the water body, it causes a moist southeasterly air current to flow towards Ethiopia (Camberlin et al, 2002; NMSA 1996). Occasionally, there are also frontal lows that either originate from the Mediterranean area or originate within the Atlantic Ocean and are swept through from west to east. These occur in association with a cold front, the intensity of which depends on the temperature contrast ahead and behind the front. As it reaches east of Mediterranean Sea, the surface front is split into two: one front over the Arabian lowland and the other over the Sudan lowland (Gizaw, 1968). Once the surface fronts reach over the high grounds, they interact with the equatorial systems and produce abundant rains over the northern, northeastern, central parts of Ethiopia and the escarpments. Sometimes when the low-level westerly trough penetrates along the Rift Valley, the rainfall activity could linger for some days.

The relationship between the Ethiopian rainfall during Belg and the tropical cyclones over the southwest Indian Ocean indicates that low/high frequency of the cyclones resulted in excess/deficit rainfall (Shanko et al, 1998).

The meridional arm of the ITCZ also contributes for the rainfall activity over East Africa. Hence, it produces rainfall during February/March over south west of Ethiopia (Kassahun, 1987).

The formation of intense and frequent tropical disturbances over the southeast Indian Ocean occurs simultaneously with Belg and Kiremt rainfall deficiency in Ethiopia (Bekele, 1992).

3. Among the systems that control the weather activity during Kiremt (the main rainy season) include:

A) The northward propagation of ITCZ as well as the formation of heat lows over the Sahara and Arabian landmasses (Korecha et al, 2007). ITCZ attains a peak position of 15°N and 15°S during July and January, respectively (Asnani, 2005). The airflow is dominated by zones of convergence in the low pressure systems accompanied by the oscillatory ITCZ extending from West Africa through Ethiopia towards India (NMSA Vol.1, 1996). There is convergence between the air stream of African southwest monsoons diverted from the south Atlantic southeast trades and the Indian southwest monsoon on the Ethiopian highlands, especially on the western, central and eastern high grounds, resulting in heavy rainfall over the region (Gizaw, 1968).

B) Formation of subtropical high pressure systems over the Azores, St. Helena, and Mascarene. The position and strength of these systems, especially the St. Helena and Mascarene, influence the moisture flux and the rainfall over Ethiopia (Kassahun, 1987). A boundary zone defined by the confluence of Atlantic/Congo and Indian Ocean air streams extends northwards along western part of Ethiopia. The rainfall activity decreases significantly in Ethiopia when the St. Helena High is weak or the boundary is displaced westwards (Kassahun, 1987).

C) The East African Low Level Jet (EALLJ) induces abundant moist air from the Southern Indian Ocean towards the high grounds of Ethiopia. Besides, there is southwesterly moisture flow from the equatorial Atlantic and Congo Basin area.

D) Tropical Easterly Jet (TEJ), which is located at the boundary of the southern and northern Hadley Cells at around 200mb, is among the systems that are most influential to the circulations in Africa (Camberlin 1997) and its formation enhances the rainfall over Ethiopia (Kassahun, 1987). Besides, the dry spells over central Ethiopia are directly related to the strength of the TEJ (Segele and Lamb 2005). A positive relationship between Sahel monsoon and strength as well as position of TEJ was identified by Hastenrath (2000). TEJ also facilitates the development of summer storm

when low level conditions are fulfilled (Gissila et al, 2004). The initial source of this jet is the Tibetan Plateau. Its development and persistence also play a great role in enhancing wide spread rains over the major rain-getting regions of northeastern Africa during the summer months (<http://orca.rsmas.miami.edu/classes/mpo551/mike//tej.html>).

2.2 ETHIOPIA RAINFALL AND GLOBAL TELECONNECTION FEATURES

Drought has been recurrent over many parts of the globe. But it is a very frequent catastrophic phenomenon over the sub-tropical regions. In Ethiopia, these situations have occurred in 1972, 1984, 1987, 1994 and 1999/2000. We will discuss the relationship between the rain-bearing systems of Ethiopia and the SST of Pacific, Atlantic and Indian Oceans, respectively.

2.2.1 PACIFIC OCEAN

Various studies have revealed the relationship between ENSO and Ethiopian rainfall and atmospheric systems (Bekele, 1993).

The principal cause of drought is asserted to be the fluctuation of the global atmospheric circulation, which is triggered by the SST anomalies occurring during ENSO events. These phenomena have significant impact on the displacement and weakening of the rain-producing mechanisms in Ethiopia (Haile, 1988).

A comparative study of a drought year (1972) and a normal rainfall year (1967) over the global tropics for the boreal summer months revealed that for a drought year we have (1) a weaker TEJ, (2) a weaker Tibetan high, and (3) a southeastward shift of the major circulation patterns as well as of several dynamic parameters (Krishnamurti and Kanamitsu, 1981).

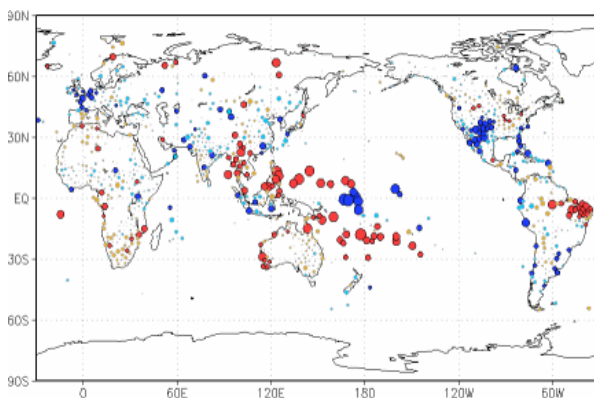
Similarly, the major rain-producing mechanism in Ethiopia and its vicinity - the ITCZ - was found to be weak, shallow, and shifted southeastward in drought years (Kruzhkova, 1981; Lamb, 1978). The findings of a case study of seasonal forecasts in Ethiopia are also consistent with the above-mentioned results (Haile, 1987). These and other findings confirm that the fluctuations of atmospheric circulation, which are sometimes triggered by SST anomalies in the equatorial Pacific (ENSO) have significant impacts on the position, magnitude, and intensity of the rain-bearing systems in Ethiopia.

The above-mentioned changes of the rain-bearing systems frequently caused meteorological, agricultural, and hydrological drought. However, the 1982-83 El Niño, which was by far the most intense one, did not produce a very dry Kiremt (Ward and Yeshanew, 1990).

June-September rainfall over the Ethiopian highlands is positively correlated to the equatorial East Pacific sea level pressure and the southern oscillation index, and negatively correlated to SST over the tropical eastern Pacific Ocean as expected, confirming again that El Niño-southern oscillation episodes are associated with below-average June-September rainfall over the Ethiopian Highlands (Seleshi and Zanke, 2004).

When looking at the effects of El Niño during March-May, more rains than normal occur. During June-August, drought over northeastern Africa is present (Figure 2).

(a) March-May



(b) June-August

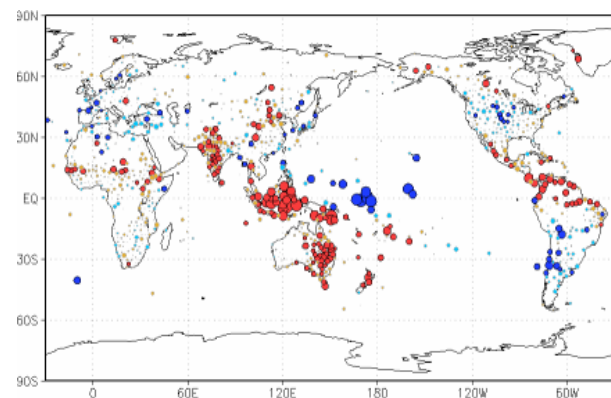


Figure 2: Effects of El Niño for the world weather during (a) March-May and (b) June-August. Blue circles indicate that during El Niño there was, on average, more rain than normal, red circles indicate drought. La Niña has the opposite effect in almost all locations. The size of the circles is a measure of the strength of the relationship (<http://www.knmi.nl/research/oceanography/enso/effects/>).

In summary, we can say that ENSO events may not be the only cause of meteorological drought in Ethiopia. However, the SST anomalies occurring during ENSO events are believed to trigger the fluctuation of the global atmospheric circulation. The impact of the ENSO on the rainfall pattern for different seasons of Ethiopia is summarized in Appendix 1 (Korecha et al, 2001; NMSA, Vol. 1, 1996).

2.2.2 ATLANTIC OCEAN

The decline of rainfall in eastern, south and south-western Ethiopia over the period approximately from 1986 to 2002 is related to the corresponding persistent warming of the South Atlantic Ocean. The sea-surface temperature (SST) over the tropical eastern Pacific Ocean is not significantly correlated with the main rainfall of the semi-arid lowland areas of eastern, southern, and southwestern Ethiopia, except at marginal zones in transition to the Ethiopian Highlands (Seleshi and Zanke, 2004).

2.2.3 INDIAN OCEAN

The variability of African rainfall is statistically related to both Pacific and Indian oceans, but the variability in the two oceans is also related. While the SST variability of the tropical Pacific exerts some influence over the African region, it is the atmospheric response to the Indian Ocean variability that is essential for simulating the correct rainfall response over eastern, central, and southern Africa. Analysis of the dynamical response(s) seen in the numerical experiments and in the observations indicate that the Pacific and Indian Ocean have a competing influence over the Indian Ocean/African region. This competition is related to the influence of the two oceans on the Walker circulation and the consequences of that variability on low-level fluxes of moisture over central and southern Africa (Hastenrath and Polzin, 2003).

Comparison of the wind anomalies that develop during extreme Indian Ocean dipole or Zonal mode (IOZM) events with those that develop during weaker (moderate) events shows that strong easterly anomalies in the northern-central Indian ocean are a persistent feature of extreme, but not of moderate, IOZM years. It is suggested that these anomalies weaken the westerly flow that normally transports moisture away from the African continent, out over the Indian Ocean. Thus, during extreme IOZM years, rainfall is enhanced over east Africa and reduced in the central and eastern Indian Ocean basin (Emily and Julia, 2002).

It is also shown that the IOZM cannot be viewed in isolation from the El Nino-Southern Oscillation (ENSO). Instead it is postulated that in some years, a strong ENSO forcing can predispose the Indian Ocean coupled system to an IOZM event and is therefore a contributory factor in extreme

East African rainfall. The results of this study imply that the relationship between El Nino and the IOZM explains the previously described association between El Nino and high East African rainfall. Thus, understanding the way that ENSO drives Indian Ocean dynamics may aid the development of predictive scenarios for East African climate that could have significant economic implications (Emily and Julia, 2002).

Over the last few decades, the Indian Ocean has warmed by over 1K which resulted in a weakening of the large scale Indian monsoon circulation because of the reduction in land-sea temperature contrast (Sperber et al. 2000).

3. DATA AND METHODOLOGY

The area has been divided into three rainfall regimes (Zone A-C, Figure 3). Zone-A is from 8°-15°N and 33°-38°E which contains northwestern and western Ethiopia as well as adjoining areas of Sudan. The main rainy season for this place is during boreal summer from June to September (Kiremt). The second zone, Zone-B, is within 8°-15°N and 38°-43°E. Northern, northeastern, eastern and central Ethiopia as well as parts of Eritrea and Red sea are included in this zone. For most parts of this area, the main rainy season is also from June to September and the second short rainy season (Belg) from March to May. The third Zone, Zone-C, is from 3°-8°N and 33°-48°E which encompasses southwestern, southern and southeastern Ethiopia as well as adjoining areas of Somalia, Kenya and Uganda. The main rainy season is from March to May and has also short rains from September to November. Besides, northwestern and northern parts of this zone also receive rain during JJA.

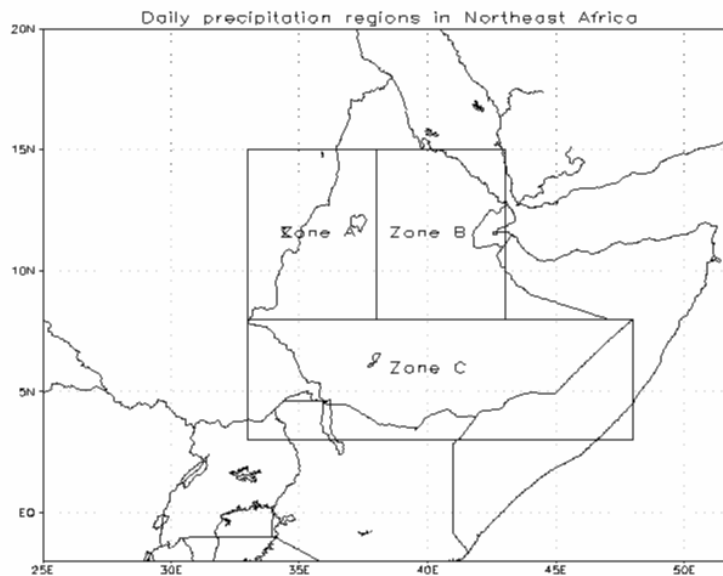


Figure 3: Location of Zones used for the study

Decadal rainfall data from the ERA-40 model output for the three regimes has been used. By subtracting the mean 1958-2001 decadal value from each decade, the anomalies are constructed. Each of the 10% extreme minimum and maximum anomalies has been identified. Then for each zone, the systems that are controlling the rainfall activity have been analyzed for the period where the extremes recorded. Hence, it will be possible to see how the extremes are formed. Next their

frequency in the future is assessed by analyzing scenario runs of GFDL and CCCma model output in each regime.

4. DATA ANALYSIS AND RESULTS

Each zone has different rainy season and rain-bearing systems. Hence, first an analysis will be presented for the Kiremt (JJAS) which is the main rainy season for Zone-A and Zone-B. Then Belg (MAM) which is the second rainy season for zone-B and the main rainy season for Zone-C.

4.1 JUNE TO SEPTEMBER

Based on the long year mean rainfall distribution (Korecha et al, 2001) especially over Ethiopia, for the month of June, northwestern, western and southwestern portions of Ethiopia, which covers nearly half of zone-A, receives 100-300mm of rainfall decreasing northwards. For zone-B, except the adjoining areas of zone-A and parts of central and eastern Ethiopia which receive 40-120mm, most of the area is dry under normal condition. The rainfall activity covers most areas of this zone from mid July onwards.

During July the rainfall activity further intensifies and expands to the northern and northeastern portions of the country. Hence, zone-A receives up to 400mm and zone-B 40-300mm. The rainfall activity is weak over the lowland areas of northeastern portions of zone-B.

During August, which is one of the peak months of the season, the rainfall activity is more or less similar to the month of July for both zones.

During the month of September the rainfall activity starts to weaken as a result of the retreat of ITCZ back to the south. Hence, zone-A receives 150-300mm and it ceases over northeastern lowlands of zone-B. Besides, up to 120mm of rainfall is recorded over northern half and southeastern portions of zone-B.

For zone-C, parts of the zone, like southwestern portions of Ethiopia, receive rainfall for more than 9 months. For JJA, except this area, the southern and southeastern parts of Ethiopia are dry under

normal conditions and nearly all places will get from 5-200mm in September. The lowlands of southern and southeastern Ethiopia receive small amounts of rainfall during September (5-10mm).

Zone-A and Zone-B receive rainfall during Kiremt. In order to see the relationship between the extreme dry/wet decades with the main rain bearing systems, the anomalous wet and dry decades have been calculated using 1958-2001 mean rainfall from ERA-40 reanalysis data. As can be seen in Figures 4 and 6 below, for most of the years up to 1970's, the anomaly is positive especially for July and August which are the peak months of the season. Later it shows a negative anomaly for most of the years throughout the season. It looks the same for Zone-B as can be seen in Figure 5 and 6. And for the month of June, it is dry under normal condition. So the anomaly is most of the time positive.

The top 10% wet and dry anomalous decades have been selected for each month and season. Figure 6 below shows the anomalous wet and dry decades for the months June-September for zone-A and zone-B, respectively. For zone-B, all the dry anomalies are in the third and first decades for July and September, respectively which are the onset and cessation decades of the lowland areas of the zone.

As can be seen in Table 2, 90-96% of the wet anomalous decades are found in the period 1958-1979. And 80-82% of the dry anomalous decades occur in 1980-2001 for both zones.

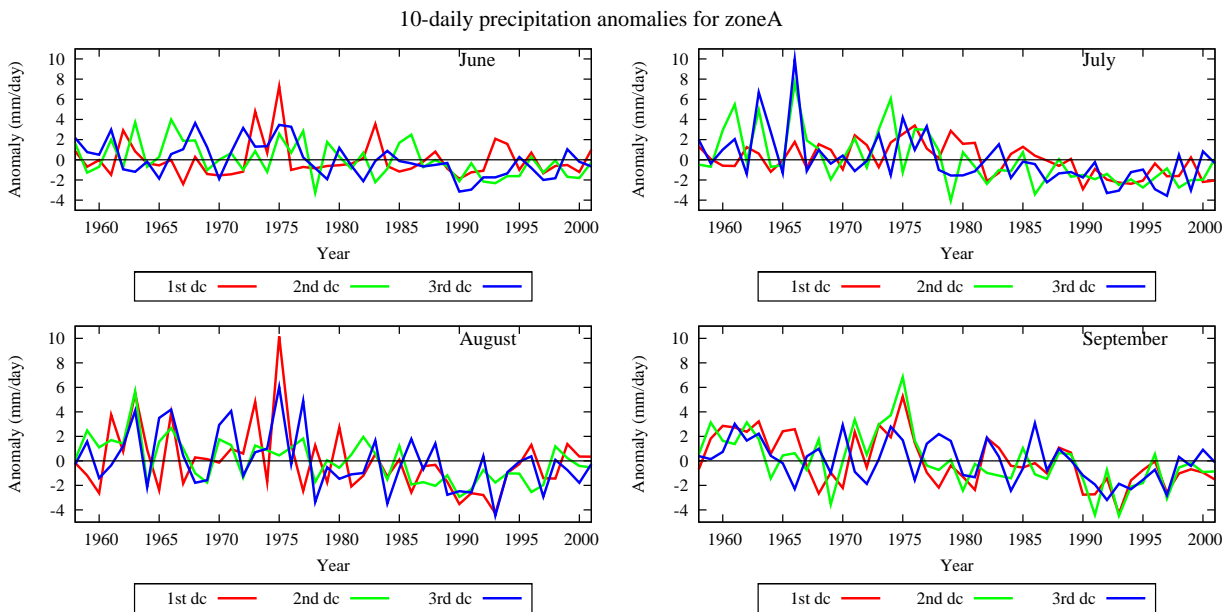


Figure 4: Time series of JJAS precipitation anomaly for Zone-A

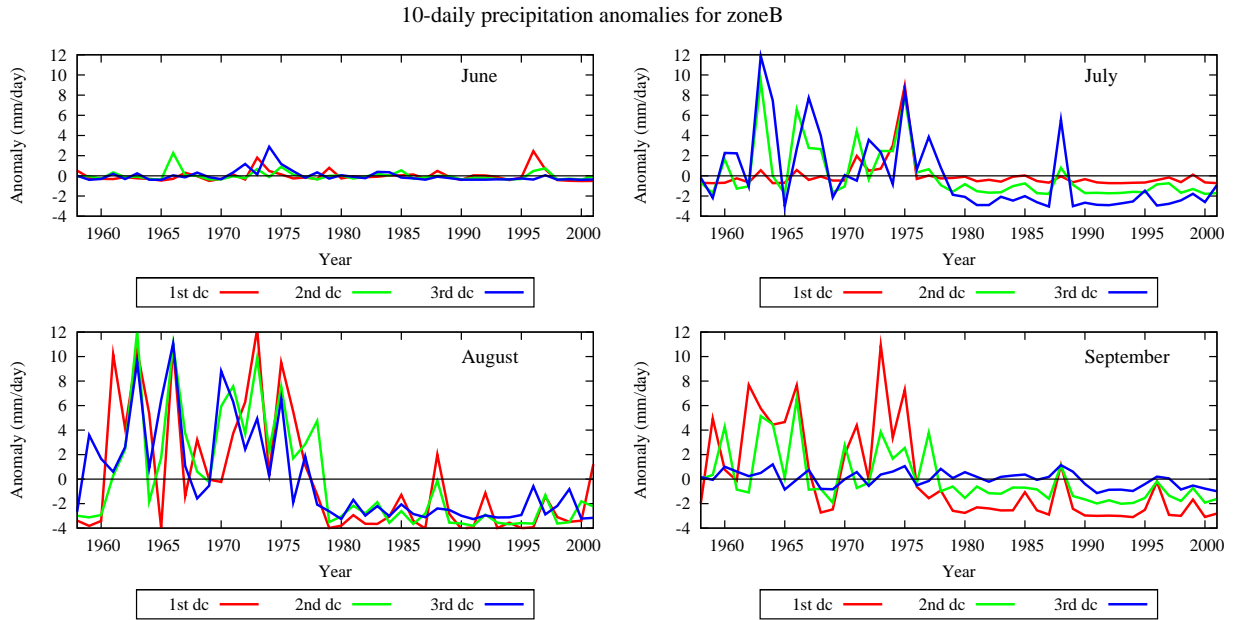


Figure 5: Time series of JJAS precipitation anomaly for Zone-B

Table 2: Summary of the frequency of wet and dry anomalies from 1958-2001

| Year | Zone-A | | | | Zone-B | | | |
|---------|-----------|-----|-------|-----|--------|-----|-------|-----|
| | Wet(JJAS) | | Dry | | Wet | | Dry | |
| | # Dec * | % | # Dec | % | # Dec | % | # Dec | % |
| 1958-79 | 50 | 96% | 9 | 17% | 47 | 90% | 10 | 19% |
| 1980-01 | 2 | 4% | 43 | 83% | 5 | 10% | 42 | 81% |

* Number of decades

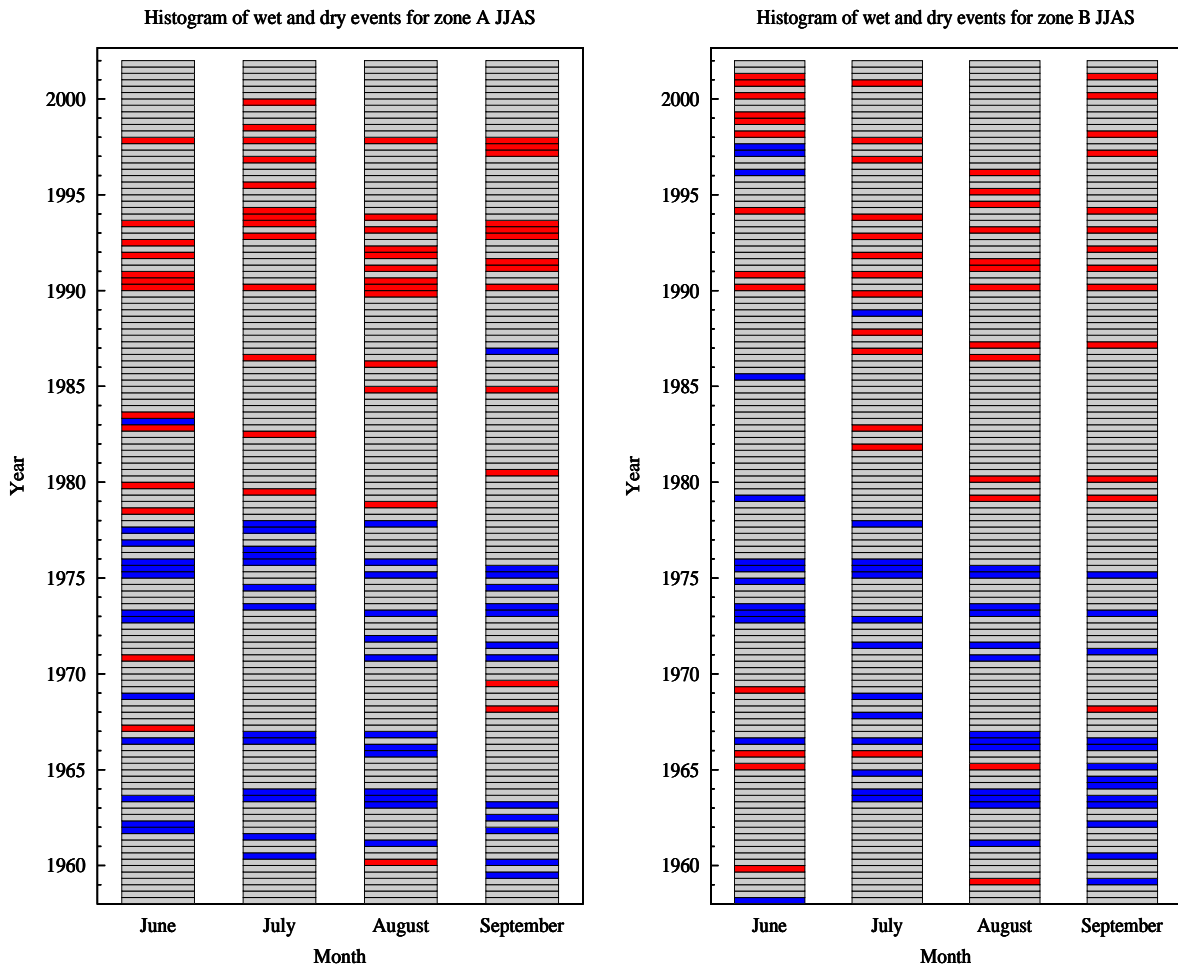


Figure 6: Histogram of JJAS decadal precipitation anomaly for Zone-A and Zone-B, respectively (red rows show dry decades and blue rows show wet decades)

4.1.1 TREND OF SYSTEMS THAT GOVERN THE RAINFALL ACTIVITY OVER THE REGION DURING THE EXTREME WET AND DRY DECADES

During JJAS the main sources of moisture are Mascarene and St Helena high pressure systems from the Indian and Atlantic Oceans, respectively. The intensity and position of these pressure systems as well as the intensity of the EALLJ have a controlling effect on the moisture entering the northeastern Africa region. The dynamic conditions like the divergence at 200mb, ITCZ and TEJ as well as the current and 3-month lag ENSO condition have also direct or indirect impact on the weather activity over the area.

Decadal mean pressure anomalies (hpa) for Macarena (20°-35°S, 30°-60°E) and St Helena's (20°-35°S, 10°W-20°E) high pressure system have been obtained from ERA-40 model output. Besides,

the anomaly of the divergence (s^{-1}) at 200mb level has been analyzed for the area which corresponds to zone-A and zone-B. For the EALLJ, the anomaly of the v-component and u-component of the wind (ms^{-1}) at 850mb for the area $8^{\circ}S-8^{\circ}N$, $38^{\circ}-48^{\circ}E$ and $4^{\circ}-14^{\circ}N$, $38^{\circ}-60^{\circ}E$, respectively have been analyzed. These anomalies have been integrated for the top 10% anomalous wet and dry decades. Besides, the current as well as the 3-month lag value of the anomaly of the Nino 3.4 region ($^{\circ}C$) has been matched to the anomalous wet and dry decades of the season. The summary of the percentage of anomalies of these systems being negative, positive and neutral in the case of ENSO for zone-A and zone-B during JJAS is displayed in Appendix 2.

In order to locate the position and intensity of the ITCZ and TEJ, using ERA-40 reanalysis data, the divergence at 925hpa and the u-component of the wind at 200hpa, respectively have been analyzed. Then the mean value within the zone $32^{\circ}E-48^{\circ}E$ has been plotted from the equator to $30^{\circ}N$ (Figure 9-11). The condition of each system is discussed below.

MASCARENE

The Mascarene high pressure system has a positive anomaly during the onset and cessation of the season (June and September) for the wet decades of zone-A and zone-B. However, during July and August most of the decades have a negative anomaly, the peak months of the season. For the dry decades, the Mascarene high pressure system anomaly is positive in more than half of the decades during the season (JJAS) for zone-A and zone-B.

A stream line analysis at 850mb shows that for most of the wet decades the centre of the Mascarene high pressure system is centered over the ocean in between $30^{\circ}-50^{\circ}E$. However, for most of the dry decades, it was either well elongated east-west, centered over the land or the centre is far from $50^{\circ}E$ (Appendix 2).

ST HELENA

The St Helena high pressure system for the wet decades of zone-A has a positive anomaly in more than half of the decades during most of the time. For zone-B, most of the decades show negative anomalies of the St Helena high pressure systems. For the dry decades, the St Helena high pressure system shows most of the time that more than half of the decades have positive anomaly for zone-A (Appendix 2).

From the stream line analysis at 850mb, for most of the wet decades there is formation of heat lows over the Sudan area around 25°-30°E and Arabian lowlands. The heat low west of 10°E did not have a direct impact on the incursion of moisture as it is far from northeastern Africa. For most of the dry decades, the heat low was centered in between 15°-25°E and will have an impact on diverting the moisture that was coming from the Congo basin area towards the northeastern Africa. Besides, there is a formation of cyclones over the Gulf of Guinea for most of the driest decades and this will have a direct impact on intrusion of moisture from the Atlantic Ocean. An example of the streamline analysis at 850hpa is shown in Figure 7 for one of the wettest and driest decades, respectively.

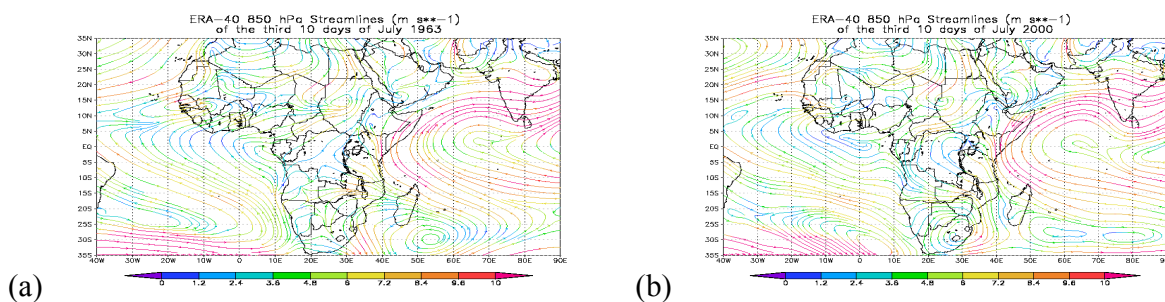


Figure 7: Streamline analysis at 850hpa for one of (a) the wettest and (b) driest decades

DIVERGENCE, V & U-COMPONENT OF EALLJ

During July and August the change in the intensity of the high pressure systems, where moisture is coming from, doesn't have more contribution for the extreme dry conditions. The means of transport (the v-component of the EALLJ) and the dynamic condition mainly the divergence at 200hpa have more correlations with the extremes.

The v-component of the EALLJ has positive/negative anomaly for most of the decades during the wet/dry decades of the season for zone-A and zone-B. June is not the rainy season for most of the area for zone-B.

The u-component of the EALLJ has a positive anomaly for more than half of the decades during the wet decades of the season for zone-A. During the dry decades, it has a positive anomaly for most of the decades during July and August and negative anomaly for more than half of the decades during June and September (Appendix 2).

The divergence at 200mb shows that for the wettest/driest decades of zone-A and zone-B, most of the decades have positive/negative anomalies. An example of the divergence at 200hpa is shown in

Figure 8 for one of the wettest and driest decades, respectively.

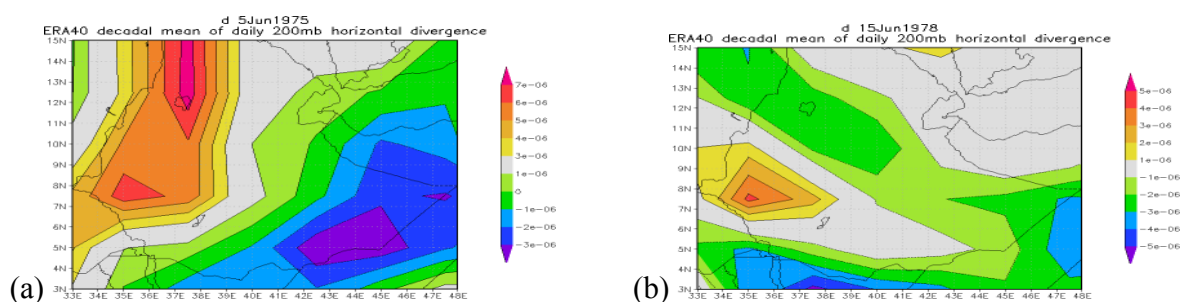


Figure 8: Divergence at 200hpa for one of (a) the wettest and (b) driest decades

ENSO

The condition of the Nino 3.4 for the anomalous decades during the month of the decade indicate that during wet decades of the season (JJAS) most of the decades for Zone-A and zone-B have negative to neutral conditions. During the dry decades of the season, most of the decades for Zone-A and zone-B have positive to neutral conditions.

The 3-month lag ENSO values during wet decades of the season shows that most of the decades are negative to neutral for zone-A and zone-B. During the dry decades of the season, most of the decades are positive to neutral and negative to neutral for zone-A and zone-B, respectively (Appendix 2).

As a summary we can say that the Nino 3.4 trend is more to neutral during June and July for the wettest decades of zone-A and tends to be more negative during August and September. For zone B, the trend is also negative to neutral, like the 3-month lag condition, from July to September. For the dry decades of both zones, it shows positive to neutral condition for most of the time. The 3-month lag ENSO condition is having negative to neutral trend for most of the decades during JJAS for the wettest decades of zone-A and zone-B and for the dry decades, positive to neutral condition is dominating. The scatterplots Nino 3.4 vs. rainfall anomaly is attached in Appendix 4.1 for the wettest and driest decades of zone A and B.

ITCZ

As can be seen from Figure 9, the ITCZ moves northwards with time starting from June and attains its peak during July and August. Then it starts to retreat back during September. Besides, the mean

position of the 10% wettest decades is either far to the north or having more convergence compared to mean position of the 10% driest decades as well as the mean monthly position for most of the time. Appendix 3 shows that the peak position and intensity is during July and August. Besides, during the wettest decades, the mean position reaches up to 20.2°N during August and the mean convergence value reaches $17 \times 10^{-6} \text{ s}^{-1}$ during July.

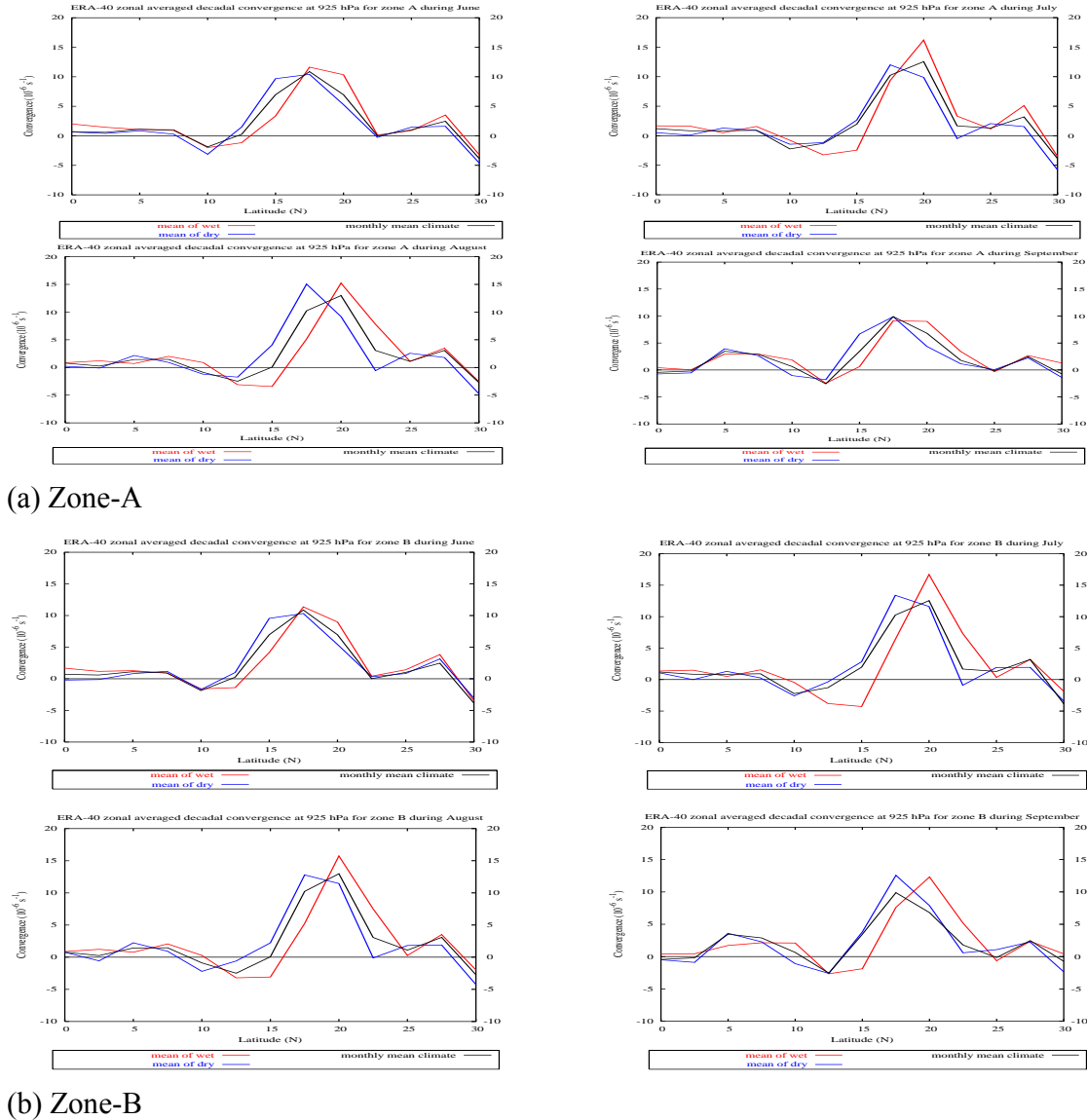


Figure 9: Wind convergence denoting the ITCZ position (30°-40°E) (a) for Zone-A and (b) for Zone-B during JJAS

TEJ

In order to see the change in the position and intensity of the jet during the wettest and driest decades, its mean value from 32°E -48°E has been taken and analyzed from the equator to 30°N.

Together with the 13 extremes, their mean position has been also plotted (Figure 10 and 11). For the wettest decades the peak reaches during July and August for zone A and B, respectively.

The position of the jet for the wettest/driest decades was south/north of 10.5°N for both zones.

The wind speed is greater than 20ms⁻¹ during July and August for both zones and the difference in strength between the wettest and driest decades is small. However, during September there is a difference of about 2ms⁻¹. Generally, the position shows a clear distinction between wet and dry conditions than the speed of the jet (Appendix 3b).

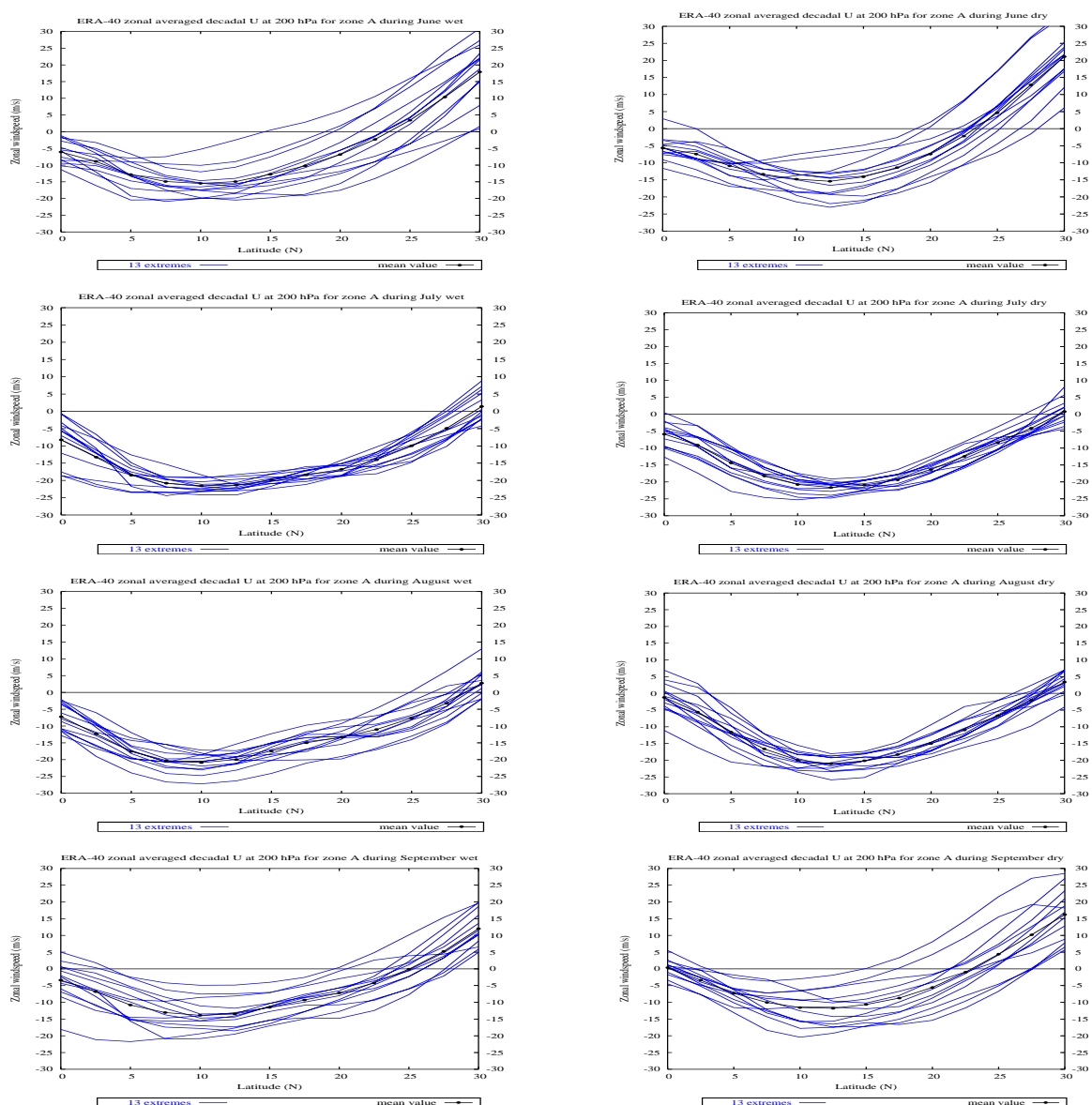


Figure 10: Zonal wind speed denoting the Position of TEJ during JJAS for zone-A for Wet (left) and Dry (right) decades. Each line represents one wet or dry episode.

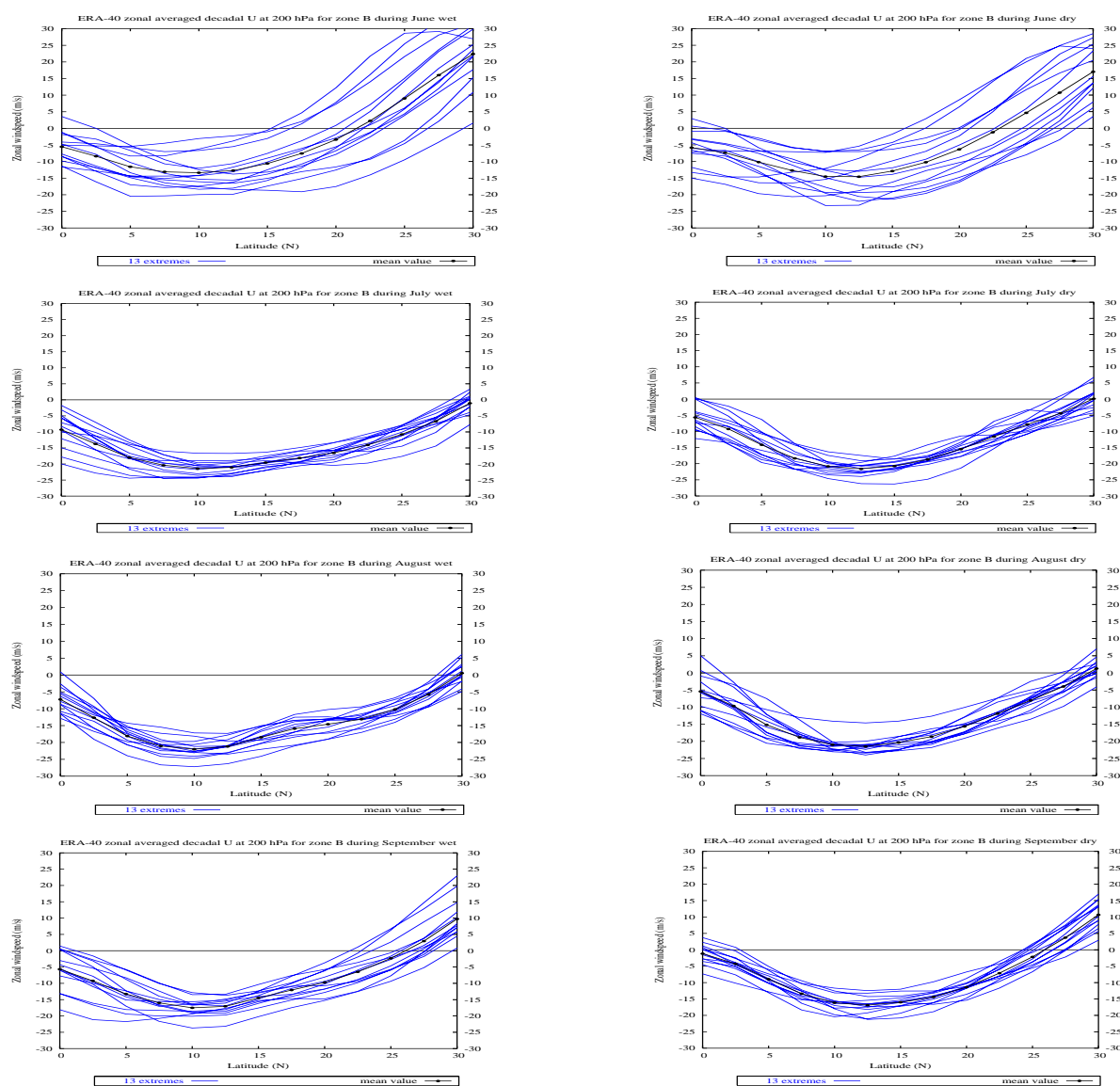


Figure 11: Zonal wind speed denoting the Position of TEJ during JJAS for zone-B for Wet (left) and Dry (right) decades.

SUMMARY OF SYSTEMS

When we study rainfall of the northeastern Africa, first we should analyze the sources of moisture and then the dynamic conditions that control the weather activity over the area. As mentioned before, the sources of moisture are from the Indian and Atlantic Ocean. The position and strength of the high pressure systems in these oceans as well as the strength of the jet which transports moisture for the case of Indian Ocean and the presence of a cyclone over Gulf of Guinea and heat

lows over Sudan/Chad will have a controlling effect for the amount of moisture that is supposed to incur from Atlantic/Congo Basin to the northeastern Africa. Besides, the incursion of moisture should be supported by the dynamic condition both on the surface and the atmosphere.

As can be seen in Appendix 2 and 3 for the wettest decades:

- The Mascarene and St. Helena high pressure systems have positive anomaly during the onset and cessation periods (June and September) and the means of transport i.e. the jet has a positive anomaly for most of the time.
- The centre of the Mascarene high pressure system is centered over the ocean 30° - 50° E.
- During July and August, the ITCZ becomes extreme north and having more convergence accompanied by a formation of heat low over the Arabian and Sudan area. This will contribute for the incursion of moisture from the Congo Basin.
- The TEJ also is more to the equator (south of 10.5° N) compared to dry decades. And the wind speed is greater than 20ms^{-1} during July and August.
- The 3-month lag ENSO and the Nino 3.4 values during most of the season show negative to neutral trend.
- The divergence at 200mb shows positive anomalies for most of the decades.

For the driest decades:

- The Mascarene and St. Helena high pressure systems show positive anomaly most of the time. The jet has negative anomaly.
- The centre of the Mascarene high pressure system is either well relaxed east-west, centered over the land or the centre is far from 50° E.
- The TEJ is far from the equator (north of 10.5° N) compared to wet decades. And the wind speed is greater than 20ms^{-1} during July and August.
- The 3-month lag ENSO and the Nino 3.4 values during most of the season show positive to neutral trend.
- The divergence at 200mb shows negative anomalies for most of the decades.
- The ITCZ becomes more to the south and less convergence compared to the wettest decades. The heat low formed over the Sudan area during the wet decades shifts to the west and is over Chad. Besides, there is a formation of cyclone over the Gulf of Guinea, which will have a direct impact on the incursion of moisture towards the area.

After looking at the condition of each system during the wet and dry decades, the most favorable condition for wet/dry episodes from June to September is discussed below:

JUNE

During June the trend in the major rain-bearing systems is summarized as follows:

- For the wettest decades the main source of moisture is from the Indian Ocean and the means of transport, the EALLJ, was also strong for most of the decades.
- As there is an imbalance between the two high pressure systems over the Indian and Atlantic Ocean, the wind from the Mascarene high pressure system crosses the southern part of Africa (becomes easterly/southeasterly). Hence, the St. Helena is not directly pumping out moisture to the northeastern Africa.
- Except southwestern portions, zone-B is dry during this time.
- The TEJ also is more to the equator compared to dry decades. However, the speed is less than 20ms^{-1} during this month.
- The 3-month lag ENSO and the Nino 3.4 values show negative to neutral trend for most of the decades.
- The divergence at 200mb shows positive anomalies for most of the decades.
- The ITCZ becomes more to the north and having strong convergence for the wettest decades compared to the driest decades.

For the driest decades:

- For the driest decades, even if the moisture source is having more positive anomaly, either the means of transport or one of the dynamic conditions like divergence at 200mb, tend to have more negative anomaly.
- The TEJ is far from the equator (north of 10.5°N) compared to wet decades. However, the speed is less than 20ms^{-1} during this month.
- The 3-month lag ENSO and the Nino 3.4 values show positive to neutral trend for most of the decades.
- The divergence at 200mb shows negative anomalies for most of the decades.
- The ITCZ becomes more to the south and less convergence compared to the wettest decades.

JULY

During July:

- For the wettest decades the sources of moisture are both from the Indian Ocean and Atlantic/Congo basin and the means of transport, the EALLJ, was also strong for most of the decades.
- The incursion of moisture from the St. Helena/Congo basin increases as the ITCZ is moving further north and there is a formation of heat lows over Sudan and Arabian land during the wettest decades.
- The rainfall activity expands from southwestern to the remaining portions of zone-B starting from mid-July.
- The TEJ also is more to the equator for the wettest compared to dry decades. Besides, the speed becomes greater than 20ms^{-1} both for the wettest and driest decades with a maximum of 22ms^{-1} .
- The ITCZ becomes more to the north (up to 20°N) and having strong convergence for the wettest decades compared to the driest decades.
- The heat low over Sudan shifts west to Chad and cyclones are formed over Gulf of Guinea especially during the driest decades of zone-B.

AUGUST

During August:

- The heat low over Sudan shifts west to Chad and cyclones are formed over Gulf of Guinea especially during the driest decades of zone-A.
- The TEJ also is more to the equator for the wettest compared to dry decades. Besides, the speed becomes greater than 20ms^{-1} both for the wettest and driest decades with a maximum of 22.3ms^{-1} .
- August is the time where the ITCZ reaches the peak up to 20.2°N and becomes more to the north and having strong convergence for the wettest decades compared to the driest decades.

SEPTEMBER

During September:

- The incursion of moisture from the St. Helena/Congo basin starts to decrease as the ITCZ retreats to the south.

- The TEJ also is more to the equator for the wettest compared to dry decades. However, it weakens and becomes less than 20ms^{-1} both for the wettest and driest decades.
- As September is the time where the ITCZ starts to retreat, there is a relative weakening and retreating and it becomes more to the north and having strong convergence for the wettest decades compared to the driest decades.
- As the retreat of the ITCZ is faster, the rainfall activity first ceases over the northeastern and eastern portions of zone-B around the first decade of September.

4.2 MARCH TO MAY

Among the zones that receive rainfall during this period include zone-B and zone-C. MAM is the short and long rainy season for zone-B and zone-C, respectively.

Based on the long year mean rainfall distribution (Korecha et al, 2001) especially over Ethiopia: For the month of March, zone-B receives 40-120 mm of rainfall with a decrease as we move towards northern and northeastern Ethiopia. Except southeastern lowlands, the remaining areas of zone-C receive 40-120mm of rainfall.

During April, over zone-C the rainfall activity intensifies and covers most parts of the zone especially over Ethiopia and it ranges from 40-200mm.

May is a transition month from Belg (short rainy season) to Kiremt (long rainy season) and the rainfall activity significantly decreases over most parts of zone-B. It continues, however, in a similar manner like April over zone-C.

In order to see the relationship between the extreme dry/wet decades with the main rain bearing systems, the anomalous wet and dry decades have been calculated using 1958-2001 mean rainfall value from the ERA40 reanalysis data. Figure 12 and 13 below shows the trend of the anomalous wet and dry decades for zone-B and zone-C.

The top 10% wet and dry anomalous decades have been selected for each month and season. Figure 12 below shows the anomalous wet and dry decades for the months MAM for zone-B and zone-C. For zone-B, all the dry anomalies are in the third decade during March. During April and May, most of the dry anomalies are in the first decade. For zone-C, most of the dry anomalies are in the

third decade during March.

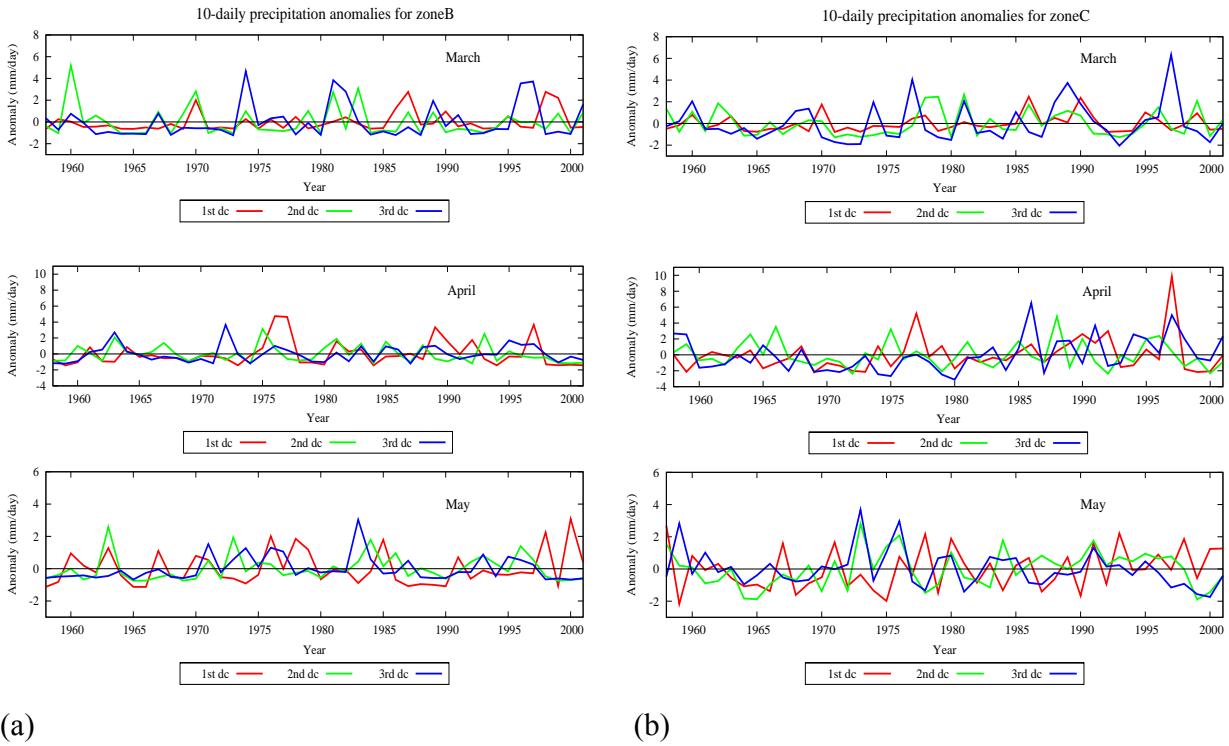


Figure 12: Time series of MAM precipitation anomaly for (a) Zone-B and (b) Zone-C

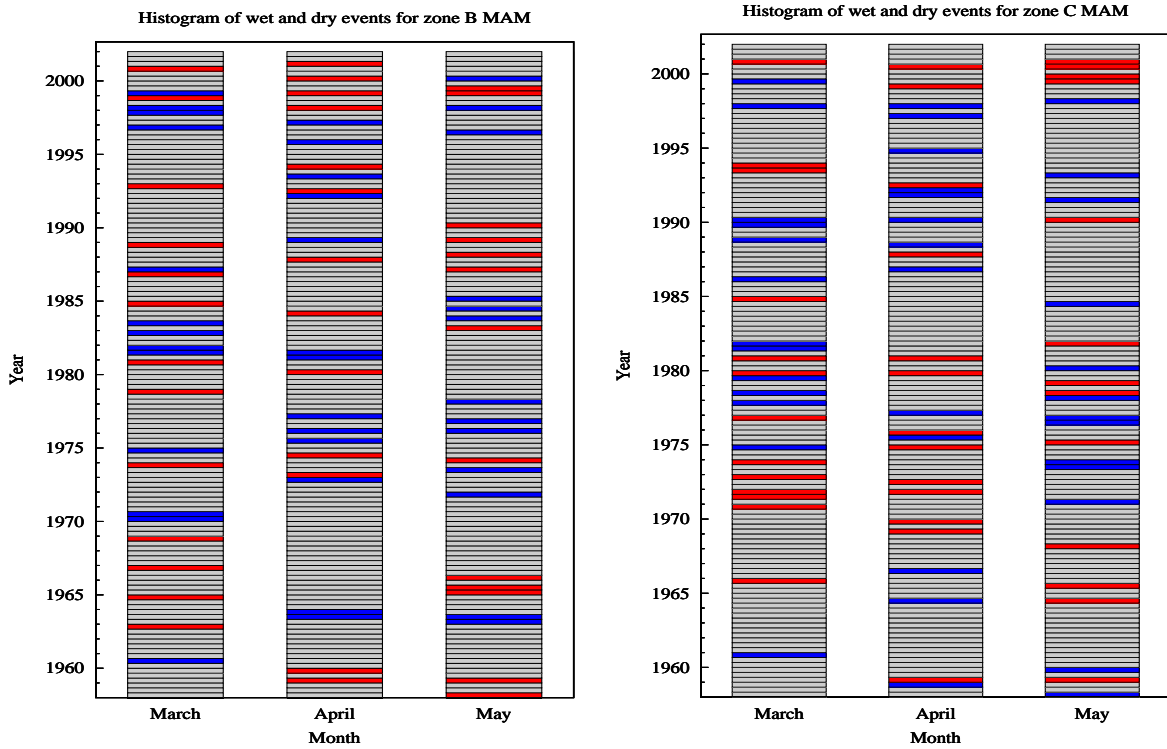


Figure 13: Histogram of MAM decadal precipitation anomaly for Zone-B and Zone-C, respectively (red rows show dry decades and blue rows show wet decades)

4.2.1 TREND OF SYSTEMS THAT GOVERN THE RAINFALL ACTIVITY OVER THE REGION DURING THE EXTREME WET AND DRY DECADES

During MAM the main source of moisture is from the Arabian high pressure system from the Indian Ocean. The position of this pressure system has a controlling effect on the moisture entering to the northeastern Africa region. Besides, the formation of the cycles over the southwestern/eastern Indian Ocean will affect the incursion of moisture. The extra-tropical trough, which is migrating from west to east, is also among the dynamic conditions which contribute for the rainfall activity over the region. The current and 3-month lag ENSO condition have also direct or indirect impact for the weather activity over the area.

In order to see the position of the Arabian high pressure system, the direction of the wind and also whether cyclones are formed and diverting the moisture, a streamline analysis has been carried out at 850mb using ERA-40 data. Besides, to look for the position of the extra tropical trough, a streamline analysis has been done at 500mb for the northern hemisphere, which covers from the equator to 60°N and from 40°W to 70°E. These have been integrated to the top 10% anomalies wet and dry decades. Besides, the current as well as the 3-month lag value of the anomaly of the Nino 3.4 region (°C) has been matched to the anomalous wet and dry decades of the season. The summary of these negative and positive anomalies for zone-B and zone-C during MAM is displayed in Appendix 5.

ARABIAN HIGH

The streamline analysis at 850mb shows that the Arabian high pressure system for most of the wettest decades is situated centered over the ocean and the wind is directed as easterly/southeasterly. In some cases it is centered over the Arabian land but well relaxed and extends to the Indian Ocean with the easterly/southeasterly wind directed towards northeastern Africa.

For most of the driest decades of the two zones, the Arabian high pressure system is centered over the land and is relaxed north-south and hence the wind is northeasterly/northerly. If centered over the ocean, it is far from northeastern Africa and is diverted by the frequent occurrence of lows/cyclones over the Indian Ocean. Figure 14 below shows sample streamline analysis at 850mb for one of the wettest and the driest decades.

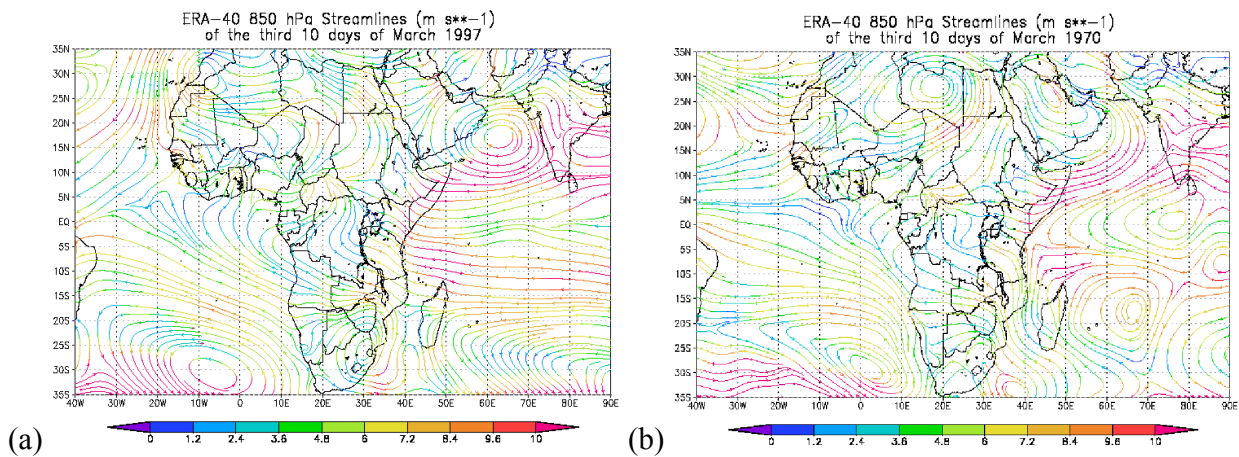


Figure 14: Streamline analysis at 850hpa for one of (a) the wettest and (b) driest decades

EXTRATROPICAL TROUGH

During this period the rainfall activity is mostly from warm stratified clouds. If there is moisture incurring to the area and is supported by the dynamic condition till 500mb, the chance of getting rainfall is maximum. When the extra-tropical trough migrates from west to east and reaches around 40°E it interacts with the meridional arm of the ITCZ and pushes the Arabian high towards the Indian Ocean and result in incursion of moisture towards the area.

The streamline analysis at 500mb shows that for most of the wettest decades the trough is over the region from 30°-50°E and well relaxed. This results also the high pressure system to be pushed to the Indian Ocean and hence additional moisture source for the region at this level.

For most of the driest decades, the region is under the influence of a high pressure system and hence further development is inhibited irrespective of the surface condition. Figure 15 below shows sample streamline analysis at 500mb for one of the wettest and the driest decades.

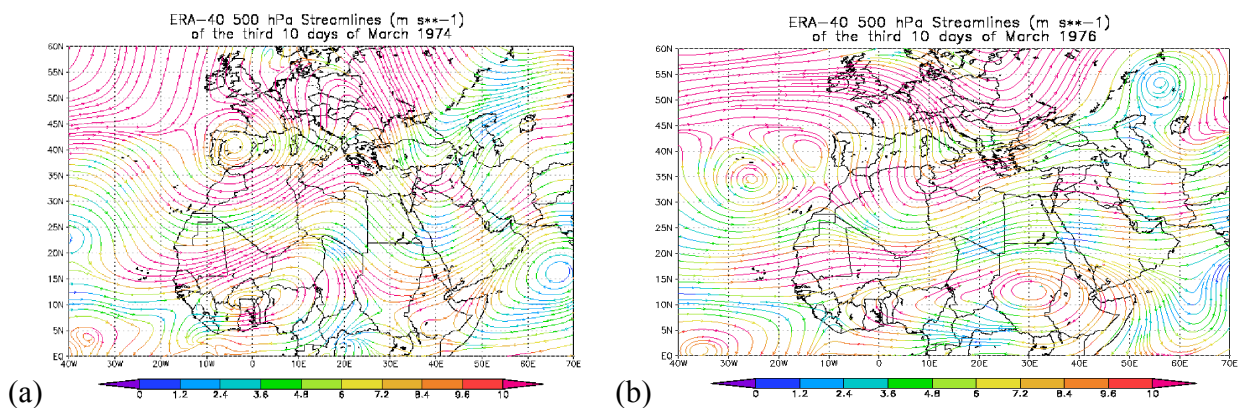


Figure 15: Streamline analysis at 500hpa for one of (a) the wettest and (b) driest decades

ENSO

The monthly anomaly of Nino 3.4 for the anomalous wet and dry decades indicate that during the season (MAM) most of the decades for zone-B and zone-C have negative to neutral conditions.

The ENSO values during wet decades of the season based on the 3-month lag ENSO condition, shows that most of the decades are under negative to neutral conditions for zone-B. For zone-C, most of the decades are under positive to neutral conditions. During the dry decades of the season, most of the decades are under negative to neutral conditions for zone-C (Appendix 5).

As a summary we can say that the Nino 3.4 trend is more negative to neutral for the wettest decades of zone-B. For zone C, the trend is negative to neutral, like the lag condition, except during April which resembles more positive to neutral condition. For the dry decades of both zones, it shows negative to neutral condition during May, which is a transition month from Belg to Kiremt. The 3-month lag ENSO condition is having positive to neutral trend for most of the decades during March and April for the wettest decades of zone-B and during May it shows negative to neutral for most of the decades. For zone-C, it is positive to neutral most of the time. For the dry decades, negative to neutral condition is dominating most of the time for zone-C. The scatterplots Nino 3.4 vs. rainfall anomaly is attached in Appendix 4.2 for the wettest and driest decades of zone B and C.

5. CLIMATE CHANGE

The energy balance of the climate system is controlled by the changes in the atmospheric abundance of greenhouse gases and aerosols, in solar radiation and in land surface properties. The climate of the northeastern Africa, especially rainfall, shows a remarkable fluctuation for the last decades which affects the different sectors. Hence, understanding the future extremes will alleviate this problem. Rainfall observation anomalies from ERA-40 and the scenario runs from the geophysical fluid dynamics laboratory (GFDL) and the Canadian Center for Climate modeling and analysis (CCCma) have been used for this purpose.

The Intergovernmental Panel on Climate Change (IPCC) does review scientific, technical and socio- economic information which are necessary for the understanding of climate change, its potential impacts and options for adaptation and mitigation. After the third assessment report (TAR) in 2001, the records have been improved, ranges of observations have been expanded and there are improvements in the simulation of many aspects of climate and its variability. Hence in the fourth assessment report (AR4) larger number of simulations is available from a broader range of models. Combining additional feedback from observations provide a quantitative basis for estimating likelihoods for many aspects of climate change. In the model simulations a range of possible future idealized emission or concentration assumptions have been considered (Summary for policy makers, in the IPCC Fourth Assessment Report (AR4), <http://www.ipcc-wg1>).

The climate models used to reproduce observed features of recent climate and past climate changes report are based on well established physical principles. Atmosphere-Ocean General Circulation Models (AOGCMs) give reliable quantitative estimates of future climate change more at continental and larger scales and there is more confidence in the estimates of temperature than precipitation (Climate Models and their Evaluation, in the IPCC Fourth Assessment Report, <http://www.ipcc-wg1>).

Even if there is insufficient feedback for future projections like the vegetation feedbacks, dust aerosol productions and possible land surface modification in the global models, there is likelihood to an increase in annual rainfall over East Africa (Regional Climate Projections, in the IPCC AR4, <http://www.ipcc-wg1>).

Future climate prediction of models reliability is evaluated based on its simulation of the current climate. Poor model skill in simulating present climate implies that certain physical or dynamical processes have been misrepresented. In the fourth Assessment report 23 models were considered to investigate historical and future climate changes. Accuracy in simulating the seasonally varying pattern of precipitation for models increases when they correctly simulate a number of processes (e.g., evapotranspiration, condensation, transport) that are difficult to evaluate at a global scale.

As most AOGCMs have coarse resolution and large scale systematic errors, and extreme events tend to be short lived and have smaller spatial scales, the intensity, frequency and distribution of extreme precipitation are less well simulated. With this constraint, two scenario runs, GFDL and CCCMA, have been analyzed for the three zones used in this study.

The CCCma has developed a number of climate simulation models for climate prediction; study of climate change and variability, and to have a better understanding of the various processes which govern our climate system (<http://www.cccma.ec.gc.ca>). The third generation coupled global climate model (CGCM3) versions CGCM3.1 (T47) and CGCM3.1 (T63) have been used in the IPCC fourth assessment report (AR4).

After the GFDL R30 and R15 experimental studies in 2004 a new family of GFDL models (the CM2.x family) was first used to conduct climate research. These models are being used to topics focusing on decadal-to-centennial time scale issues (including multi-century control experiments and climate change projections), as well as to seasonal-to-interannual problems, such as El Niño research and experimental forecasts (<http://www.gfdl.noaa.gov/>).

The GFDL CM2.0 and GFDL CM2.1 models were used by the Intergovernmental Panel on Climate Change (IPCC) for their fourth assessment report (AR4). They have surface grid of spatial resolution roughly $2.0^\circ \times 2.5^\circ$ and 24 levels in the vertical.

Looking the past and future climate trend using CCCma and GFDL models and comparing with ERA-40 reanalysis data has been done for the three zones used in this study. Figure 16 shows the future trend of precipitation for zone-A and B during August for both models. The results are as follows:

- Both CCCma and GFDL models have a consistent trend, however, the variability is higher for

the CCCma than the GFDL.

- A decreasing and increasing trend during the onset (June) and the cessation (September), respectively especially for the Kiremt season.
- The monomodal rainfall trend for zone-A becomes bimodal with peaks during July and September.
- For zone-B, it will have another peak during October which was dry during the current climate.
- Hence, the seasonality is not well represented in these models.

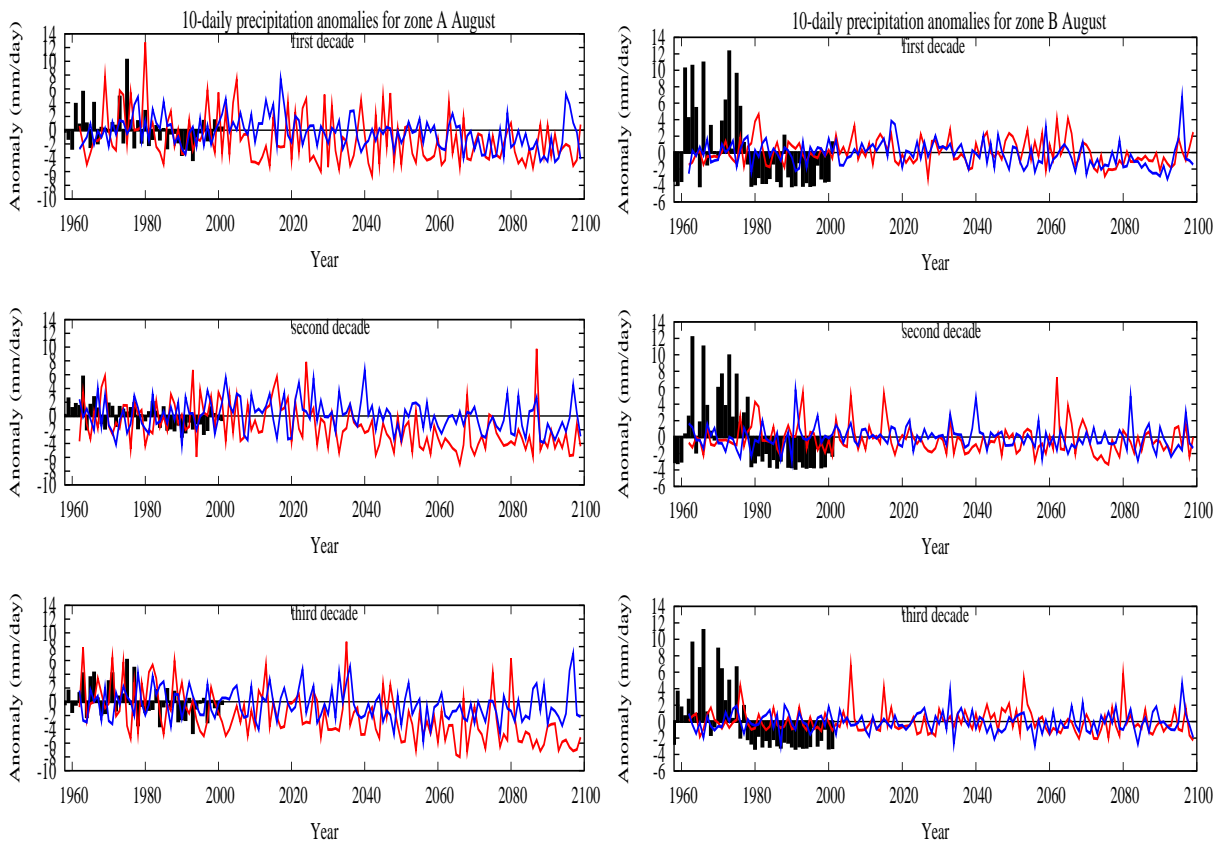


Figure 16: Decadal Rainfall anomalies with respect to 1960-2000 during August for zone-A and Zone-B ERA-40 (black box), ccma (red) and gfdl (blue line).

In the previous chapters we have seen the main systems which govern the weather and those which have significant correlation with the extremes. When looking at the future trend of the climate, the trend of the main systems should be analyzed. Hence the next step for this work will be looking at the trend of these systems for the coming century using different model outputs.

6. DISCUSSION AND CONCLUSIONS

This study assesses the distribution of anomalies in decadal bases and the condition of the main rain-bearing systems during these decades as well as the expected changes in the frequency and intensity of extreme rainfall induced by climate change.

The northeastern Africa (Ethiopia) has been divided into three homogeneous rainfall regimes (Zone A-C). The seasonal classification of the region, especially over Ethiopia, is from February to May, June to September and October to January, called Belg, Kiremt and Bega, respectively. Here, more emphasis is given to the Kiremt (JJAS) and Belg (MAM) seasons.

Anomalous wet and dry decades were identified using ERA-40 data. The condition of the main rain bearing systems during these decades has been assessed and from this result systems which favor more for the extremes have been detected. Among the systems that control the weather activity in the region include ITCZ, TEJ, EALLJ, ENSO as well as Mascarena, St. Helena, Azores and Arabian High pressure systems. Then using GFDL and CCCMA, simulations were analyzed.

There is large decadal variability in the occurrence of extreme rainfall events. During Kiremt season, 90-96% wet anomalous were mostly situated in the 1958-1979 time range. The dry anomalous decades were mostly found in 1980-2001 for both zone-A and -B. During Belg, all the dry anomalies are in the third decade during March for zone-B. During April and May, most of the dry anomalies are in the first decade. For zone-C, most of the dry anomalies are in the third decade during March.

For the wettest decades during Kiremt, the Mascarena and St. Helena high pressure systems (centered over the ocean) have positive anomaly during the onset and cessation periods (June and September) and the means of transport (the jet) has a positive anomaly most of the time. For the driest decades, the Mascarena and St. Helena high pressure systems (centered either over the land or stretched east-west) show positive anomaly most of the time. However, the jet has negative anomaly. The 3-month lag and current Nino 3.4 during most of the season show negative to neutral and positive to neutral conditions for most of the wettest and driest decades, respectively.

During July and August, the ITCZ reaches an extremely northern position and has more

convergence accompanied by a formation of a heat low over the Arabian and Sudan area. This contributes to the incursion of moisture from the Congo Basin. The TEJ is shifted to the equator (south of 10.5°N) compared to dry decades. During driest decades, the heat low formed over the Sudan area shifts to the west and is over Chad. Besides, there is a formation of cyclone over the Gulf of Guinea, which affects the incursion of moisture towards the area.

During Belg (MAM), the Arabian high pressure system for most of the wettest decades is situated centered over the ocean and the wind is directed as easterly/southeasterly. In some cases it is centered over the Arabian land but well relaxed and extends to the Indian Ocean with the easterly/southeasterly wind directed towards northeastern Africa. The extra tropical trough at 500mb is over the region from 30° - 50°E and well relaxed which results also the high pressure system to be pushed to the Indian Ocean and hence additional moisture source for the region at this level. The ENSO values during wet decades of the season based on the 3-month lag ENSO condition, shows that most of the decades are under negative to neutral conditions for zone-B. For zone-C, most of the decades are under positive to neutral conditions. The Nino 3.4 trend is more negative to neutral for the wettest and driest decades of both zones. This implies that Nino 3.4 condition is not a clear indication for anomalies but the lag gives more signal.

For the driest decades during MAM, the Arabian high pressure system is centered over the land and is relaxed north-south and hence the wind is northeasterly/northerly. If centered over the ocean, it is far from northeastern Africa and is diverted by the frequent occurrence of lows/cyclones over the Indian Ocean. The region is under the influence of a high pressure system at 500mb and hence further development is inhibited irrespective of the surface condition.

The sources of moisture, the means of transport and the dynamic conditions are important to generate a wet anomaly. During the driest decades these conditions are not fulfilled. The future scenario runs from GFDL and CCCma indicate that both models have a consistent trend. However, as most models have limitations, even the seasonality is not well represented in both models. Hence, emphasis should be given to include various parameters missing in these models to improve their outputs. Besides, the future trend of the systems that govern the extremes needs to be analyzed.

ACKNOWLEDGMENT

I would like to express my profound heart-felt gratitude and appreciation to my supervisors Prof. B. van den Hurk and Dr. G. J van Oldenborgh for their invaluable advice, reviews and comments during the writing of this paper. Also thanks to Bas de Boer for his kind assistance in the data analysis.

I wish to express my unbounded sincere thanks to Nuffic, the Netherlands Organization for International Cooperation in Higher Education for awarding me fellowship that enables me to undergo this study and also to KNMI for allowing me to use all the facilities during my stay.

I am also indebted to my employer, National Meteorological Agency (NMA), A.A, Ethiopia, for granting me study leave for the duration of the study.

Last, but not least, I extend my special gratitude to my beloved wife Adanech W/Michael who, besides offering moral support during the course of the study, patiently took care of our children, Lydia and Biruk, while I was away in the Netherlands for two years.

REFERENCES

- Asnani, G. (2005). Tropical Meteorology, Volume 1. Praveen Printing Press, revised edition.
- Bekele, F., 1993: Probability of Drought Occurrence under Different Events. NMSA mimeo. Addis Ababa, Ethiopia: NMSA.
- Black E. and Slingo J.M., 2002: An Observational Study of the Relationship between Excessively Strong Short Rains in Coastal East Africa and Indian Ocean SST. *Monthly Weather Review*, 131, 74-94.
- Coppola, E., Grimes, D.I.F., Verdecchia, M., Visconti, G., 2005: Validation of improved TAMANN neural network for operational satellite-derived rainfall estimation in Africa. Submitted to *J. App. Met.*
- Camberlin P., 1997: Rainfall anomalies in the source region of the Nile and their connection with the Indian summer monsoon. *J. Climate*, 10, 1380–1392.
- Camberlin P., and Philippon, N. (2002): The East African March-May Rainy season: Associated Atmospheric dynamics and predictability over the 1968-97 period. *J. Climate*, 15, 1002-1019.
- Gissila, T., Black, E., Grimes, D., and Slingo, J., 2004: Seasonal forecasting of the Ethiopian summer rains. *International Journal of Climatology*, 24, 1345-1358.
- Haile, T., 1987: A case study of seasonal forecasts in Ethiopia. In: WMO RAI (Africa) Seminar on Modern Weather Forecasting (Part II), 30 November-4 December 1987. Addis Ababa, Ethiopia, 53-83.
- Haile, T., 1988: Causes and characteristics of drought in Ethiopia. *Ethiopian Journal of Agricultural Science*, 10, 85-97
- Hastenrath S., 1991: *Climate Dynamics of the Tropics*. Kluwer Academic Publishers, 488 pp.
- Hastenrath S., 2000: Interannual and longer term variability of upper-air circulation over the tropical Atlantic and West Africa in boreal summer. *Int. J. Climatol.*, 20, 1415–1430.
- Hastenrath S. and Polzin D., 2003: Dynamics of the surface wind field over the equatorial Indian Ocean. *Q. J. R. Meteorol. Soc.* (2004), 130, pp. 503–517.
- Kassahun B., 1987: Weather systems over Ethiopia. Proc. First Tech. Conf. on Meteorological Research in Eastern and Southern Africa, Nairobi, Kenya, UCAR, 53–57.
- Korecha D., and Babu A., 2001: *National Climate Atlas of Ethiopia*. NMSA, A.A, Ethiopia.
- Korecha D. and Barnston A. G., 2007: Predictability of June–September Rainfall in Ethiopia. *Amer. Meteor. Soc.*, 135, 625-650.
- Krishnamurti, T.N., and M. Kanamitsu, 1981: Northern summer planetary-scale monsoons during

drought and normal rainfall months. *Monsoon Dynamics*, 19-48.

Kruzhkova, T.S., 1981: On certain features of the atmospheric circulation in periods of drought. In: R.P. Pearce (Ed.), *Tropical Droughts, Meteorological Aspects and Implication for Agriculture*. *Gidrometeorostat: Moscow*, 49-55.

Lamb, P.J., 1978: Case study of tropical Atlantic surface circulation patterns during recent sub-Saharan weather anomalies, 1976 and 1986. *Monthly Weather Review*, 106, 482-491.

NMSA, 1996: Climatic and agroclimatic resources of Ethiopia. National Meteorological Services Agency of Ethiopia, *Meteorological Research Report Series*, Vol. 1, No. 1, 1–137.

Regional Climate Projections, IPCC Fourth Assessment Report, <http://www.ipcc-wg1>.

Segele Z. T., and P. J. Lamb, 2005: Characterization and variability of Kiremt rainy season over Ethiopia. *Meteor. Atmos. Phys.*, 89, 153–180. Find this article online

Shanko D., and P. Camberlin, 1998: The effect of the southwest Indian Ocean tropical cyclones on Ethiopian drought. *Int. J. Climatol.*, 18, 1373–1378. Find this article online

Sileshi Y., and G. R. Demarée, 1995: Rainfall variability in the Ethiopian and Eritrean highlands and its links with the Southern Oscillation Index. *J. Biogeogr.*, 22, 945–952. Find this article online

Sperber, K.R., Slingo, J.M. & Annamalia, H. 2000: Predictability and the relationship between subseasonal and interannual variability during the Asian summer monsoon. *Q.J.R. Meteorol.Soc.* 126, 2545-2574.

Tefera, G., Grimes, D., Black, E., and O'Neill, A., 2007: Evaluation of Reanalysis Rainfall Estimates over Ethiopia

Ward, M., and A. Yeshanew, 1990: Worldwide sea surface temperature and Kiremt rains in Ethiopia. NMSA mimeo. Addis Ababa, Ethiopia: NMSA.

<http://orca.rsmas.miami.edu/classes/mpo551/mike//tej.html>

<http://agrifish.jrc.it/bulletins.htm>

<http://www.knmi.nl/research/oceanography/enso/effects/>

<http://www.cccma.ec.gc.ca/>

<http://www.gfdl.noaa.gov/>

Appendix 1: Impact of ENSO for different seasons over Ethiopia

| Cases | DJF | MAM | JJA | SON |
|---|---|--|---|---|
| Weak El Niño | Av-A. Av. Rain over S. & SE Ethiopia compared to moderate el Niño | | | |
| La Niña | Negatively affects the seasonal rains | | | |
| Non episodic El Niño | Dry | -Larger rainfall over the area than La Niña or normal years -A. Av. rains for most area during moderate to strong El Niño | | |
| Non episodic | | Enhanced rainfall irrespective of the preceding event Deficient rainfall | | |
| El Niño/ La Niña continue from the preceding season | | | | |
| El Niño follows a normal | | Better rain over some regions | | |
| Decay of El Niño & emerging of La Niña | | | -better rains over most of western half, NE & Southern Ethiopia | |
| El Niño during MAM followed by a normal case | | | -A. Av. Rains concentrate only over S & SE regions -deficient over the rest of country | |
| La Niña occurs after normal events | | | -N & SW areas receive better rains than W & NE sectors Deficient over Various parts | |
| Rest of ENSO/normal cases | | | | Most regions receive near average rains |
| El Niño persist from JJA through SON | | | | S & Western margins get A. Av. rains |
| El Niño dies out & replaced by normal events | | | | Above Av. rains over Central, E, S & SE |
| Emerging of El Niño following normal events | | | | W. & NW parts hardly benefit |
| La Niña continue with in the season | | | | |
| Emergence of La Niña | | | | -Enhances at places of S. highlands & N. extremes -deficient over E & western portions |
| No episodic event in the preceding season | | | | Normal rainfall |

Appendix 2: Summary of the anomaly percentage for some of the rain bearing systems during the wettest and driest decades from June to September and for zone A and B

| Month | Zone | Anomaly (%) | Wettest decades | | | | | | Driest decades | | | | | | | |
|-------|------|-------------|-----------------|------|---------|-------|-------|-------------|----------------|-----|------|---------|-------|-------|-------------|----------------|
| | | | Mas | St.H | DIV-200 | U-LLJ | V-LLJ | ENSO (lag) | ENSO (current) | Mas | St.H | DIV-200 | U-LLJ | V-LLJ | ENSO (lag) | ENSO (current) |
| June | A | positive | *85 | 54 | 85 | 62 | 62 | 15 | 31 | 54 | 54 | 15 | 46 | 38 | 23 | 46 |
| | | Negative | 15 | 46 | 15 | 38 | 38 | 46 | 31 | 46 | 46 | 85 | 54 | 62 | 0 | 0 |
| | | Neutral | | | | | | 39 | 38 | | | | | | 77 | 54 |
| | B | positive | 69 | 46 | 69 | 46 | 38 | 15 | 38 | 77 | 38 | 15 | 46 | 69 | 31 | 31 |
| | | Negative | 31 | 54 | 31 | 54 | 62 | 31 | 38 | 23 | 62 | 85 | 54 | 31 | 23 | 38 |
| | | Neutral | | | | | | 54 | 23 | | | | | | 46 | 31 |
| July | A | positive | 31 | 38 | 77 | 54 | 62 | 0 | 15 | 69 | 69 | 0 | 77 | 8 | 46 | 38 |
| | | Negative | 69 | 62 | 23 | 46 | 38 | 38 | 15 | 31 | 31 | 100 | 23 | 92 | 8 | 15 |
| | | Neutral | | | | | | 62 | 69 | | | | | | 46 | 46 |
| | B | positive | 15 | 23 | 100 | 31 | 62 | 8 | 23 | 62 | 62 | 0 | 62 | 23 | 39 | 54 |
| | | Negative | 85 | 77 | 0 | 69 | 38 | 46 | 38 | 38 | 38 | 100 | 38 | 77 | 15 | 0 |
| | | Neutral | | | | | | 46 | 38 | | | | | | 46 | 46 |
| Aug. | A | positive | 15 | 54 | 100 | 54 | 77 | 8 | 31 | 62 | 69 | 8 | 85 | 15 | 46 | 31 |
| | | Negative | 85 | 46 | 0 | 46 | 23 | 31 | 38 | 38 | 31 | 92 | 15 | 85 | 0 | 7 |
| | | Neutral | | | | | | 62 | 31 | | | | | | 54 | 62 |
| | B | positive | 23 | 38 | 92 | 62 | 92 | 0 | 23 | 38 | 46 | 0 | 31 | 15 | 46 | 46 |
| | | Negative | 77 | 62 | 8 | 38 | 8 | 38 | 46 | 62 | 54 | 100 | 69 | 85 | 0 | 0 |
| | | Neutral | | | | | | 62 | 31 | | | | | | 54 | 54 |
| Sept. | A | positive | 62 | 54 | 92 | 54 | 54 | 8 | 15 | 69 | 38 | 0 | 38 | 23 | 54 | 31 |
| | | Negative | 38 | 46 | 8 | 46 | 46 | 54 | 77 | 31 | 62 | 100 | 62 | 77 | 0 | 0 |
| | | Neutral | | | | | | 38 | 8 | | | | | | 46 | 69 |
| | B | positive | 77 | 54 | 92 | 62 | 85 | 23 | 23 | 77 | 54 | 0 | 54 | 23 | 38 | 23 |
| | | Negative | 23 | 46 | 8 | 38 | 15 | 38 | 54 | 23 | 46 | 100 | 46 | 77 | 8 | 8 |
| | | Neutral | | | | | | 38 | 23 | | | | | | 54 | 69 |
| JJAS | A | positive | | | | | | 7.7 | 23.1 | | | | | | 42.3 | 36.5 |
| | | Negative | | | | | | 42.3 | 40.4 | | | | | | 1.9 | 5.8 |
| | | Neutral | | | | | | 50 | 36.5 | | | | | | 55.8 | 57.7 |
| | B | positive | | | | | | 11.5 | 26.9 | | | | | | 38.5 | 38.5 |
| | | Negative | | | | | | 38.5 | 44.2 | | | | | | 11.5 | 11.5 |
| | | Neutral | | | | | | 50 | 28.8 | | | | | | 50.0 | 50.0 |

Note: * indicates 85% of the wettest decades have positive anomaly of Mascarene high pressure system during June for zone A.

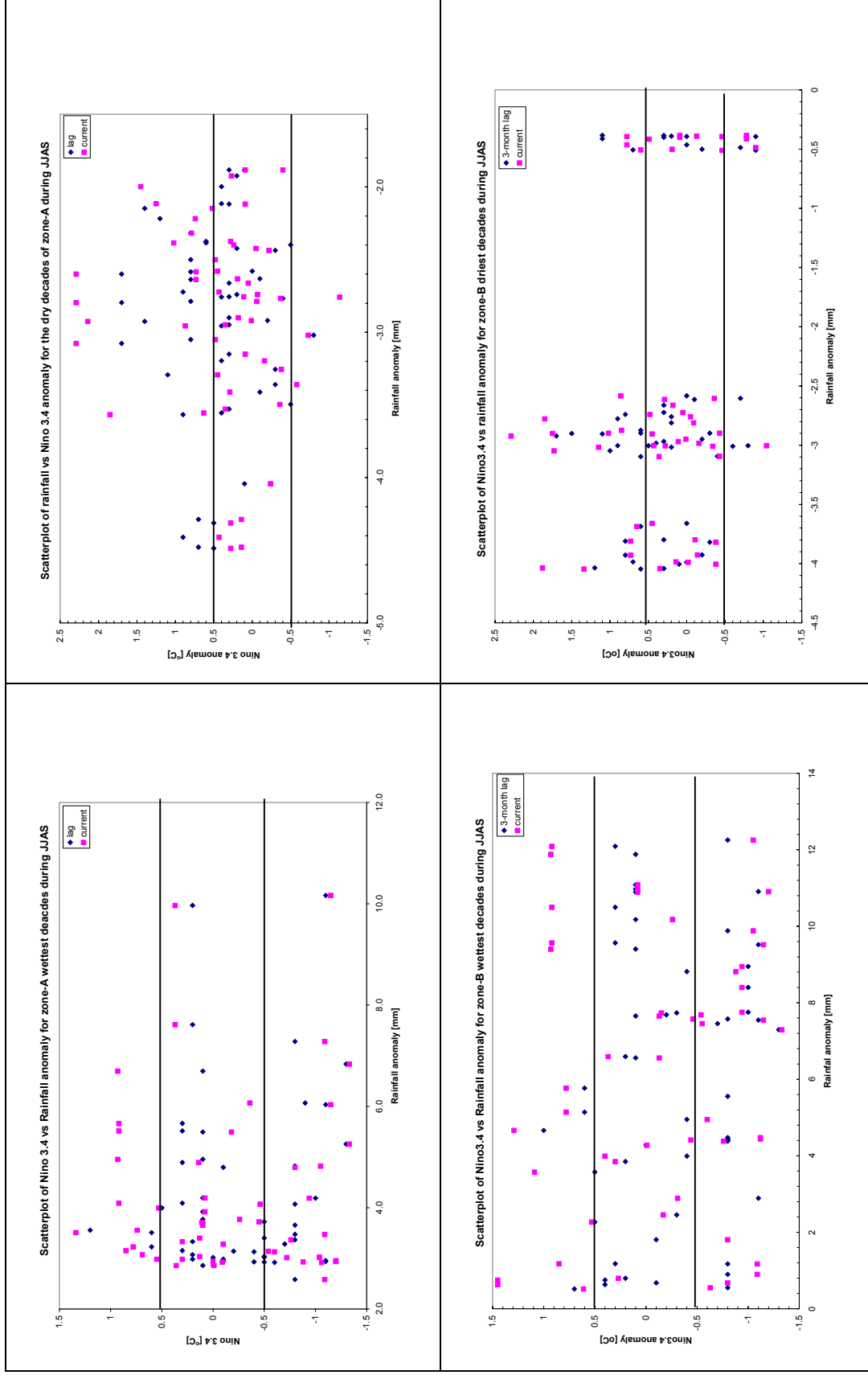
Appendix 3a: Summary of the mean position and convergence of the ITCZ

| Month | Zone-A | | | | Zone-B | | | |
|-------|---------------|---------------------------------|---------------|---------------------------------|---------------|---------------------------------|---------------|---------------------------------|
| | Wet | | Dry | | Wet | | Dry | |
| | Position (°N) | Convergence ($10^{-6}s^{-1}$) | Position (°N) | Convergence ($10^{-6}s^{-1}$) | Position (°N) | Convergence ($10^{-6}s^{-1}$) | Position (°N) | Convergence ($10^{-6}s^{-1}$) |
| June | 18.3±1.2 | 13.3±2.1 | 16.5±1.3 | 11.5±1.3 | 17.9±0.9 | 12.5±2.3 | 16.3±1.3 | 11.8±1.8 |
| July | 19.7±0.7 | 16.4±3.1 | 18.5±1.3 | 13.3±2.5 | 20±0.0 | 17±2.6 | 18.6±1.2 | 14.3±2.3 |
| Aug. | 20.2±0.7 | 15.9±3 | 17.7±0.7 | 15.2±1.7 | 20.2±0.7 | 16.3±2.8 | 18.5±1.3 | 14.6±1.6 |
| Sept. | 18.8±1.7 | 11.7±2.5 | 16.7±1.2 | 10.5±2.9 | 19.6±0.9 | 13±2.3 | 17.9±0.9 | 13±1.5 |

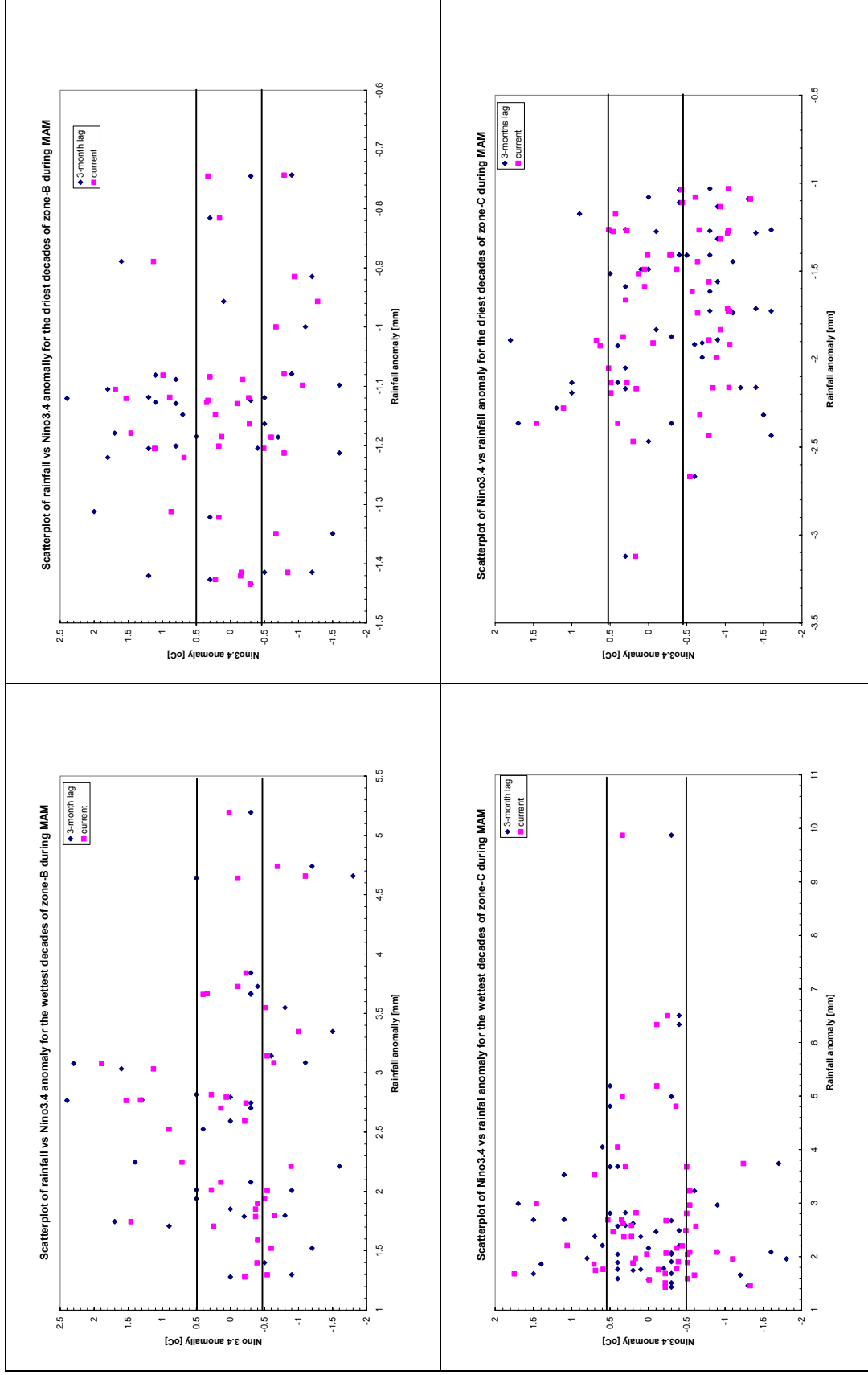
Appendix 3b: Summary of the mean speed and position of the TEJ

| Month | Zone-A | | | | Zone-B | | | |
|--------|---------------|---------------------|---------------|---------------------|---------------|---------------------|---------------|---------------------|
| | Wet | | Dry | | Wet | | Dry | |
| | Position (°N) | Speed (ms^{-1}) | Position (°N) | Speed (ms^{-1}) | Position (°N) | Speed (ms^{-1}) | Position (°N) | Speed (ms^{-1}) |
| June | 10±1.6 | 16.3±4.1 | 11.2±3 | 16.2±4.2 | 9.1±3.8 | 14.2±4.7 | 10.5±3.2 | 15.8±5.9 |
| July | 10.1±1.6 | 22±1.8 | 13±2.1 | 22±1.8 | 9.8±1.9 | 21.8±2.4 | 12.1±1.8 | 21.9±2.1 |
| August | 10±1.8 | 21.3±2.6 | 12.4±1.3 | 20.8±2.5 | 10.3±1.1 | 22.3±2.6 | 11.7±1.6 | 21.7±2.3 |
| Sept. | 9.6±2.3 | 14.5±4.9 | 11.0±2.6 | 12.5±4.8 | 9.9±2.0 | 18.1±2.9 | 11.8±1.1 | 16.9±2.9 |

Appendix 4.1: Scatterplot of Nino 3.4 vs. rainfall anomaly for Zone-A and zone-B during JJAS for the wettest and driest decades



Appendix 4.2: Scatterplot of Nino 3.4 and zone-C during MAM for the wettest and driest decades



Appendix 5: Summary of the anomaly percentage for some of the rain bearing systems (ENSO) during the wettest and driest decades from March to May and for zone A and B

| Month | Zone | Status | Wettest | | Driest | |
|-------|------|----------|-------------|---------------|-------------|---------------|
| | | | ENSO(lag) | ENSO(current) | ENSO(lag) | ENSO(current) |
| March | B | positive | 38.5 | 23.1 | 53.8 | 30.8 |
| | | negative | 23.1 | 23.1 | 30.8 | 23.1 |
| | | neutral | 38.5 | 53.8 | 15.4 | 46.2 |
| | C | positive | 23.1 | 7.7 | 15.4 | 30.8 |
| | | negative | 23.1 | 30.8 | 53.8 | 30.8 |
| | | neutral | 53.8 | 61.5 | 30.8 | 38.5 |
| April | B | positive | 23.1 | 15.4 | 30.8 | 27.3 |
| | | negative | 23.1 | 23.1 | 30.8 | 27.3 |
| | | neutral | 53.8 | 61.5 | 38.5 | 45.5 |
| | C | positive | 38.5 | 23.1 | 30.8 | 30.8 |
| | | negative | 7.7 | 15.4 | 38.5 | 38.5 |
| | | neutral | 53.8 | 61.5 | 30.8 | 30.8 |
| May | B | positive | 23.1 | 15.4 | 30.8 | 15.4 |
| | | negative | 46.2 | 46.2 | 30.8 | 38.5 |
| | | neutral | 30.8 | 38.5 | 38.5 | 46.2 |
| | C | positive | 38.5 | 23.1 | 0.0 | 0.0 |
| | | negative | 23.1 | 38.5 | 46.2 | 53.8 |
| | | neutral | 38.5 | 38.5 | 53.8 | 46.2 |
| MAM | B | positive | 28.2 | 17.9 | 38.5 | 24.3 |
| | | negative | 30.8 | 30.8 | 30.8 | 29.7 |
| | | neutral | 41.0 | 51.3 | 30.8 | 45.9 |
| | C | positive | 33.3 | 17.9 | 15.4 | 20.5 |
| | | negative | 17.9 | 28.2 | 46.2 | 41.0 |
| | | neutral | 48.7 | 53.8 | 38.5 | 38.5 |

